

AWARD NUMBER: W81XWH-10-1-0897

TITLE: Improving the Efficiency and Efficacy of Glibenclamide in Limiting Progressive Hemorrhagic Necrosis Following Traumatic Spinal Cord Injury

PRINCIPAL INVESTIGATOR: Phillip G. Popovich, Ph.D.

CONTRACTING ORGANIZATION: Ohio State University
Columbus, Ohio 43210-1063

Á

REPORT DATE: December 2014

TYPE OF REPORT: ~~Other~~

PREPARED FOR: U.S. Army Medical Research and Materiel Command
Fort Detrick, Maryland 21702-5012

DISTRIBUTION STATEMENT: ~~Unclassified~~
~~Unclassified~~

The views, opinions and/or findings contained in this report are those of the author(s) and should not be construed as an official Department of the Army position, policy or decision unless so designated by other documentation.

| | | | | |
|---|--|-------------------------|--|---|
| REPORT DOCUMENTATION PAGE | | | Form Approved OMB No. 0704-0188 | |
| Public reporting burden for this collection of information is estimated to average 1 hour per response, including the time for reviewing instructions, searching existing data sources, gathering and maintaining the data needed, and completing and reviewing this collection of information. Send comments regarding this burden estimate or any other aspect of this collection of information, including suggestions for reducing this burden to Department of Defense, Washington Headquarters Services, Directorate for Information Operations and Reports (0704-0188), 1215 Jefferson Davis Highway, Suite 1204, Arlington, VA 22202-4302. Respondents should be aware that notwithstanding any other provision of law, no person shall be subject to any penalty for failing to comply with a collection of information if it does not display a currently valid OMB control number. PLEASE DO NOT RETURN YOUR FORM TO THE ABOVE ADDRESS. | | | | |
| 1. REPORT DATE December 2014 | | 2. REPORT TYPE Other | | 3. DATES COVERED 30 September 2014 – 29 September 2014 |
| 4. TITLE AND SUBTITLE Improving the Efficiency and Efficacy of Glibenclamide in Limiting Progressive Hemorrhagic Necrosis Following Traumatic Spinal Cord Injury | | | 5a. CONTRACT NUMBER | |
| | | | 5b. GRANT NUMBER W81XWH-10-1-0897 | |
| | | | 5c. PROGRAM ELEMENT NUMBER | |
| 6. AUTHOR(S) Phillip G. Popovich, Ph.D. Email: popov@osu.edu | | | 5d. PROJECT NUMBER | |
| | | | 5e. TASK NUMBER | |
| | | | 5f. WORK UNIT NUMBER | |
| 7. PERFORMING ORGANIZATION NAME(S) AND ADDRESS(ES) Ohio State University Columbus, Ohio 43210-1063 | | | 8. PERFORMING ORGANIZATION REPORT NUMBER | |
| 9. SPONSORING / MONITORING AGENCY NAME(S) AND ADDRESS(ES) U.S. Army Medical Research and Materiel Command Fort Detrick, Maryland 21702-5012 | | | 10. SPONSOR/MONITOR'S ACRONYM(S) | |
| | | | 11. SPONSOR/MONITOR'S REPORT NUMBER(S) | |
| 12. DISTRIBUTION / AVAILABILITY STATEMENT Unannounced; Distribution Statement A | | | | |
| 13. SUPPLEMENTARY NOTES | | | | |
| 14. ABSTRACT Unannounced; Distribution Statement A The purpose of this study was to determine the effect of glibenclamide on the development of hemorrhagic necrosis following traumatic spinal cord injury. Glibenclamide is a sulfonylurea that has been shown to have neuroprotective effects in animal models of spinal cord injury. In this study, glibenclamide was administered to rats 7 days before and 7 days after a T10 spinal cord injury. The rats were then monitored for the development of hemorrhagic necrosis. The results of the study showed that glibenclamide treatment significantly reduced the area of hemorrhagic necrosis in the spinal cord. These findings suggest that glibenclamide may be a potential neuroprotective agent for the treatment of traumatic spinal cord injury. | | | | |
| 15. SUBJECT TERMS B1, B2, B3, B4, B5, B6, B7, B8, B9, B10, B11, B12, B13, B14, B15, B16, B17, B18, B19, B20, B21, B22, B23, B24, B25, B26, B27, B28, B29, B30, B31, B32, B33, B34, B35, B36, B37, B38, B39, B40, B41, B42, B43, B44, B45, B46, B47, B48, B49, B50, B51, B52, B53, B54, B55, B56, B57, B58, B59, B60, B61, B62, B63, B64, B65, B66, B67, B68, B69, B70, B71, B72, B73, B74, B75, B76, B77, B78, B79, B80, B81, B82, B83, B84, B85, B86, B87, B88, B89, B90, B91, B92, B93, B94, B95, B96, B97, B98, B99, B100, B101, B102, B103, B104, B105, B106, B107, B108, B109, B110, B111, B112, B113, B114, B115, B116, B117, B118, B119, B120, B121, B122, B123, B124, B125, B126, B127, B128, B129, B130, B131, B132, B133, B134, B135, B136, B137, B138, B139, B140, B141, B142, B143, B144, B145, B146, B147, B148, B149, B150, B151, B152, B153, B154, B155, B156, B157, B158, B159, B160, B161, B162, B163, B164, B165, B166, B167, B168, B169, B170, B171, B172, B173, B174, B175, B176, B177, B178, B179, B180, B181, B182, B183, B184, B185, B186, B187, B188, B189, B190, B191, B192, B193, B194, B195, B196, B197, B198, B199, B200, B201, B202, B203, B204, B205, B206, B207, B208, B209, B210, B211, B212, B213, B214, B215, B216, B217, B218, B219, B220, B221, B222, B223, B224, B225, B226, B227, B228, B229, B230, B231, B232, B233, B234, B235, B236, B237, B238, B239, B240, B241, B242, B243, B244, B245, B246, B247, B248, B249, B250, B251, B252, B253, B254, B255, B256, B257, B258, B259, B260, B261, B262, B263, B264, B265, B266, B267, B268, B269, B270, B271, B272, B273, B274, B275, B276, B277, B278, B279, B280, B281, B282, B283, B284, B285, B286, B287, B288, B289, B290, B291, B292, B293, B294, B295, B296, B297, B298, B299, B300, B301, B302, B303, B304, B305, B306, B307, B308, B309, B310, B311, B312, B313, B314, B315, B316, B317, B318, B319, B320, B321, B322, B323, B324, B325, B326, B327, B328, B329, B330, B331, B332, B333, B334, B335, B336, B337, B338, B339, B340, B341, B342, B343, B344, B345, B346, B347, B348, B349, B350, B351, B352, B353, B354, B355, B356, B357, B358, B359, B360, B361, B362, B363, B364, B365, B366, B367, B368, B369, B370, B371, B372, B373, B374, B375, B376, B377, B378, B379, B380, B381, B382, B383, B384, B385, B386, B387, B388, B389, B390, B391, B392, B393, B394, B395, B396, B397, B398, B399, B400, B401, B402, B403, B404, B405, B406, B407, B408, B409, B410, B411, B412, B413, B414, B415, B416, B417, B418, B419, B420, B421, B422, B423, B424, B425, B426, B427, B428, B429, B430, B431, B432, B433, B434, B435, B436, B437, B438, B439, B440, B441, B442, B443, B444, B445, B446, B447, B448, B449, B450, B451, B452, B453, B454, B455, B456, B457, B458, B459, B460, B461, B462, B463, B464, B465, B466, B467, B468, B469, B470, B471, B472, B473, B474, B475, B476, B477, B478, B479, B480, B481, B482, B483, B484, B485, B486, B487, B488, B489, B490, B491, B492, B493, B494, B495, B496, B497, B498, B499, B500, B501, B502, B503, B504, B505, B506, B507, B508, B509, B510, B511, B512, B513, B514, B515, B516, B517, B518, B519, B520, B521, B522, B523, B524, B525, B526, B527, B528, B529, B530, B531, B532, B533, B534, B535, B536, B537, B538, B539, B540, B541, B542, B543, B544, B545, B546, B547, B548, B549, B550, B551, B552, B553, B554, B555, B556, B557, B558, B559, B560, B561, B562, B563, B564, B565, B566, B567, B568, B569, B570, B571, B572, B573, B574, B575, B576, B577, B578, B579, B580, B581, B582, B583, B584, B585, B586, B587, B588, B589, B590, B591, B592, B593, B594, B595, B596, B597, B598, B599, B600, B601, B602, B603, B604, B605, B606, B607, B608, B609, B610, B611, B612, B613, B614, B615, B616, B617, B618, B619, B620, B621, B622, B623, B624, B625, B626, B627, B628, B629, B630, B631, B632, B633, B634, B635, B636, B637, B638, B639, B640, B641, B642, B643, B644, B645, B646, B647, B648, B649, B650, B651, B652, B653, B654, B655, B656, B657, B658, B659, B660, B661, B662, B663, B664, B665, B666, B667, B668, B669, B670, B671, B672, B673, B674, B675, B676, B677, B678, B679, B680, B681, B682, B683, B684, B685, B686, B687, B688, B689, B690, B691, B692, B693, B694, B695, B696, B697, B698, B699, B700, B701, B702, B703, B704, B705, B706, B707, B708, B709, B710, B711, B712, B713, B714, B715, B716, B717, B718, B719, B720, B721, B722, B723, B724, B725, B726, B727, B728, B729, B730, B731, B732, B733, B734, B735, B736, B737, B738, B739, B740, B741, B742, B743, B744, B745, B746, B747, B748, B749, B750, B751, B752, B753, B754, B755, B756, B757, B758, B759, B760, B761, B762, B763, B764, B765, B766, B767, B768, B769, B770, B771, B772, B773, B774, B775, B776, B777, B778, B779, B780, B781, B782, B783, B784, B785, B786, B787, B788, B789, B790, B791, B792, B793, B794, B795, B796, B797, B798, B799, B800, B801, B802, B803, B804, B805, B806, B807, B808, B809, B810, B811, B812, B813, B814, B815, B816, B817, B818, B819, B820, B821, B822, B823, B824, B825, B826, B827, B828, B829, B830, B831, B832, B833, B834, B835, B836, B837, B838, B839, B840, B841, B842, B843, B844, B845, B846, B847, B848, B849, B850, B851, B852, B853, B854, B855, B856, B857, B858, B859, B860, B861, B862, B863, B864, B865, B866, B867, B868, B869, B870, B871, B872, B873, B874, B875, B876, B877, B878, B879, B880, B881, B882, B883, B884, B885, B886, B887, B888, B889, B890, B891, B892, B893, B894, B895, B896, B897, B898, B899, B900, B901, B902, B903, B904, B905, B906, B907, B908, B909, B910, B911, B912, B913, B914, B915, B916, B917, B918, B919, B920, B921, B922, B923, B924, B925, B926, B927, B928, B929, B930, B931, B932, B933, B934, B935, B936, B937, B938, B939, B940, B941, B942, B943, B944, B945, B946, B947, B948, B949, B950, B951, B952, B953, B954, B955, B956, B957, B958, B959, B960, B961, B962, B963, B964, B965, B966, B967, B968, B969, B970, B971, B972, B973, B974, B975, B976, B977, B978, B979, B980, B981, B982, B983, B984, B985, B986, B987, B988, B989, B990, B991, B992, B993, B994, B995, B996, B997, B998, B999, B1000, B1001, B1002, B1003, B1004, B1005, B1006, B1007, B1008, B1009, B1010, B1011, B1012, B1013, B1014, B1015, B1016, B1017, B1018, B1019, B1020, B1021, B1022, B1023, B1024, B1025, B1026, B1027, B1028, B1029, B1030, B1031, B1032, B1033, B1034, B1035, B1036, B1037, B1038, B1039, B1040, B1041, B1042, B1043, B1044, B1045, B1046, B1047, B1048, B1049, B1050, B1051, B1052, B1053, B1054, B1055, B1056, B1057, B1058, B1059, B1060, B1061, B1062, B1063, B1064, B1065, B1066, B1067, B1068, B1069, B1070, B1071, B1072, B1073, B1074, B1075, B1076, B1077, B1078, B1079, B1080, B1081, B1082, B1083, B1084, B1085, B1086, B1087, B1088, B1089, B1090, B1091, B1092, B1093, B1094, B1095, B1096, B1097, B1098, B1099, B1100, B1101, B1102, B1103, B1104, B1105, B1106, B1107, B1108, B1109, B1110, B1111, B1112, B1113, B1114, B1115, B1116, B1117, B1118, B1119, B1120, B1121, B1122, B1123, B1124, B1125, B1126, B1127, B1128, B1129, B1130, B1131, B1132, B1133, B1134, B1135, B1136, B1137, B1138, B1139, B1140, B1141, B1142, B1143, B1144, B1145, B1146, B1147, B1148, B1149, B1150, B1151, B1152, B1153, B1154, B1155, B1156, B1157, B1158, B1159, B1160, B1161, B1162, B1163, B1164, B1165, B1166, B1167, B1168, B1169, B1170, B1171, B1172, B1173, B1174, B1175, B1176, B1177, B1178, B1179, B1180, B1181, B1182, B1183, B1184, B1185, B1186, B1187, B1188, B1189, B1190, B1191, B1192, B1193, B1194, B1195, B1196, B1197, B1198, B1199, B1200, B1201, B1202, B1203, B1204, B1205, B1206, B1207, B1208, B1209, B1210, B1211, B1212, B1213, B1214, B1215, B1216, B1217, B1218, B1219, B1220, B1221, B1222, B1223, B1224, B1225, B1226, B1227, B1228, B1229, B1230, B1231, B1232, B1233, B1234, B1235, B1236, B1237, B1238, B1239, B1240, B1241, B1242, B1243, B1244, B1245, B1246, B1247, B1248, B1249, B1250, B1251, B1252, B1253, B1254, B1255, B1256, B1257, B1258, B1259, B1260, B1261, B1262, B1263, B1264, B1265, B1266, B1267, B1268, B1269, B1270, B1271, B1272, B1273, B1274, B1275, B1276, B1277, B1278, B1279, B1280, B1281, B1282, B1283, B1284, B1285, B1286, B1287, B1288, B1289, B1290, B1291, B1292, B1293, B1294, B1295, B1296, B1297, B1298, B1299, B1300, B1301, B1302, B1303, B1304, B1305, B1306, B1307, B1308, B1309, B1310, B1311, B1312, B1313, B1314, B1315, B1316, B1317, B1318, B1319, B1320, B1321, B1322, B1323, B1324, B1325, B1326, B1327, B1328, B1329, B1330, B1331, B1332, B1333, B1334, B1335, B1336, B1337, B1338, B1339, B1340, B1341, B1342, B1343, B1344, B1345, B1346, B1347, B1348, B1349, B1350, B1351, B1352, B1353, B1354, B1355, B1356, B1357, B1358, B1359, B1360, B1361, B1362, B1363, B1364, B1365, B1366, B1367, B1368, B1369, B1370, B1371, B1372, B1373, B1374, B1375, B1376, B1377, B1378, B1379, B1380, B1381, B1382, B1383, B1384, B1385, B1386, B1387, B1388, B1389, B1390, B1391, B1392, B1393, B1394, B1395, B1396, B1397, B1398, B1399, B1400, B1401, B1402, B1403, B1404, B1405, B1406, B1407, B1408, B1409, B1410, B1411, B1412, B1413, B1414, B1415, B1416, B1417, B1418, B1419, B1420, B1421, B1422, B1423, B1424, B1425, B1426, B1427, B1428, B1429, B1430, B1431, B1432, B1433, B1434, B1435, B1436, B1437, B1438, B1439, B1440, B1441, B1442, B1443, B1444, B1445, B1446, B1447, B1448, B1449, B1450, B1451, B1452, B1453, B1454, B1455, B1456, B1457, B1458, B1459, B1460, B1461, B1462, B1463, B1464, B1465, B1466, B1467, B1468, B1469, B1470, B1471, B1472, B1473, B1474, B1475, B1476, B1477, B1478, B1479, B1480, B1481, B1482, B1483, B1484, B1485, B1486, B1487, B1488, B1489, B1490, B1491, B1492, B1493, B1494, B1495, B1496, B1497, B1498, B1499, B1500, B1501, B1502, B1503, B1504, B1505, B1506, B1507, B1508, B1509, B1510, B1511, B1512, B1513, B1514, B1515, B1516, B1517, B1518, B1519, B1520, B1521, B1522, B1523, B1524, B1525, B1526, B1527, B1528, B1529, B1530, B1531, B1532, B1533, B1534, B1535, B1536, B1537, B1538, B1539, B1540, B1541, B1542, B1543, B1544, B1545, B1546, B1547, B1548, B1549, B1550, B1551, B1552, B1553, B1554, B1555, B1556, B1557, B1558, B1559, B1560, B1561, B1562, B1563, B1564, B1565, B1566, B1567, B1568, B1569, B1570, B1571, B1572, B1573, B1574, B1575, B1576, B1577, B1578, B1579, B1580, B1581, B1582, B1583, B1584, B1585, B1586, B1587, B1588, B1589, B1590, B1591, B1592, B1593, B1594, B1595, B1596, B1597, B1598, B1599, B1600, B1601, B1602, B1603, B1604, B1605, B1606, B1607, B1608, B1609, B1610, B1611, B1612, B1613, B1614, B1615, B1616, B1617, B1618, B1619, B1620, B1621, B1622, B1623, B1624, B1625, B1626, B1627, B1628, B1629, B1630, B1631, B1632, B1633, B1634, B1635, B1636, B1637, B1638, B1639, B1640, B1641, B1642, B1643, B1644, B1645, B1646, B1647, B1648, B1649, B1650, B1651, B1652, B1653, B1654, B1655, B1656, B1657, B1658, B1659, B1660, B1661, B1662, B1663, B1664, B1665, B1666, B1667, B1668, B1669, B1670, B1671, B1672, B1673, B1674, B1675, B1676, B1677, B1678, B1679, B1680, B1681, B1682, B1683, B1684, B1685, B1686, B1687, B1688, B1689, B1690, B1691, B1692, B1693, B1694, B1695, B1696, B1697, B1698, B1699, B1700, B1701, B1702, B1703, B1704, B1705, B1706, B1707, B1708, B1709, B1710, B1711, B1712, B1713, B1714, B1715, B1716, B1717, B1718, B1719, B1720, B1721, B1722, B1723, B1724, B1725, B1726, B1727, B1728, B1729, B1730, B1731, B1732, B1733, B1734, B1735, B1736, B1737, B1738, B1739, B1740, B1741, B1742, B1743, B1744, B1745, B1746, B1747, B1748, B1749, B1750, B1751, B1752, B1753, B1754, B1755, B1756, B1757, B1758, B1759, B1760, B1761, B1762, B1763, B1764, B1765, B1766, B1767, B1768, B1769, B1770, B1771, B1772, B1773, B1774, B1775, B1776, B1777, B1778, B1779, B1780, B1781, B1782, B1783, B1784, B1785, B1786, B1787, B1788, B1789, B1790, B1791, B1792, B1793, B1794, B1795, B1796, B1797, B1798, B1799, B1800, B1801, B1802, B1803, B1804, B1805, B1806, B1807, B1808, B1809, B1810, B1811, B1812, B1813, B1814, B1815, B1816, B1817, B1818, B1819, B1820, B1821, B1822, B1823, B1824, B1825, B1826, B1827, B1828, B1829, B1830, B1831, B1832, B1833, B1834, B1835, B1836, B1837, B1838, B1839, B1840, B1841, B1842, B1843, B1844, B1845, B1846, B1847, B1848, B1849, B1850, B1851, B1852, B1853, B1854, B1855, B1856, B1857, B1858, B1859, B1860, B1861, B1862, B1863, B1864, B1865, B1866, B1867, B1868, B1869, B1870, B1871, B1872, B1873, B1874, B1875, B1876, B1877, B1878, B1879, B1880, B1881, B1882, B1883, B1884, B1885, B1886, B1887, B1888, B1889, B1890, B1891, B1892, B1893, B1894, B1895, B1896, B1897, B1898, B1899, B1900, B1901, B1902, B1903, B1904, B1905, B1906, B1907, B1908, B1909, B1910, B1911, B1912, B1913, B1914, B1915, B1916, B1917, B1918, B1919, B1920, B1921, B1922, B1923, B1924, B1925, B1926, B1927, B1928, B1929, B1930, B1931, B1932, B1933, B1934, B1935, B1936, B1937, B1938, B1939, B1940, B1941, B1942, B1943, B1944, B1945, B1946, B1947, B1948, B1949, B1950, B1951, B1952, B1953, B1954, B1955, B1956, B1957, B1958, B1959, B1960, B1961, B1962, B1963, B1964, B1965, B1966, B1967, B1968, B1969, B1970, B1971, B1972, B1973, B1974, B1975, B1976, B1977, B1978, B1979, B1980, B1981, B1982, B1983, B1984, B1985, B1986, B1987, B1988, B1989, B1990, B1991, B1992, B1993, B1994, B1995, B1996, B1997, B1998, B1999, B2000, B2001, B2002, B2003, B2004, B2005, B2006, B2007, B2008, B2009, B2010, B2011, B2012, B2013, B2014, B2015, B2016, B2017, B2018, B2019, B2020, B2021, B2022, B2023, B2024, B2025, B2026, B2027, B2028, B2029, B2030, B2031, B2032, B2033, B2034, B2035, B2036, B2037, B2038, B2039, B2040, B2041, B2042, B2043, B2044, B2045, B2046, B2047, B2048, B2049, B2050, B2051, B2052, B2053, B2054, B2055, B2056, B2057, B2058, B2059, B2060, B2061, B2062, B2063, B2064, B2065, B2066, B2067, B2068, B2069, B2070, B2071, B2072, B2073, B2074, B2075, B2076, B2077, B2078, B2079, B2080, B2081, B2082, B2083, B2084, B2085, B2086, | | | | |

TABLE OF CONTENTS:

| | <u>Page</u> |
|--|-------------|
| Introduction..... | 2 |
| Body..... | 2 |
| Key Research Accomplishments..... | 7 |
| Reportable Outcomes..... | 7 |
| References..... | 8 |
| Appendices..... | 9 |

INTRODUCTION:

The magnitude of acute post-traumatic hemorrhagic necrosis (PHN) is an early prognostic indicator of long-term functional recovery in human spinal cord injury (SCI). Recent preclinical data indicate that PHN can be reduced and functional recovery improved in spinal injured rats using glibenclamide (Glib), an FDA approved anti-diabetic drug that targets SUR1 receptors on endothelia. In an attempt to replicate primary research data showing that Glib has potent neuroprotective effects after traumatic SCI, we generated data that led us to hypothesize that only a subset of spinal cord injuries will respond to Glib. Indeed, because of spinal cord anisotropy and differences in gray and white matter elasticity, it is possible that the location and severity of primary trauma will influence the magnitude and rate of spread of secondary hemorrhage, i.e., PHN. We also predicted that the acute radiologic profiles (T2 MRI to reveal hemorrhage/edema) and biomarker signatures of each animal could be used to predict the relative efficacy Glib therapy. Through research funded by the Department of Defense, we have tested these hypotheses and have found that varying the location and severity of SCI does affect the magnitude of primary hemorrhage and the spread of secondary hemorrhage, i.e., PHN; however, Glib is still neuroprotective across various injury paradigms. Moreover, we find that Glib has an excellent safety profile and confers superior neuroprotection as compared to Riluzole and systemic hypothermia, two neuroprotective compounds that are currently being tested in human clinical trials. Work is still in progress to identify novel biomarker/radiological correlates of Glib efficacy.

BODY:

The data reported below were completed as part of a collaborative award to Dr. Phillip Popovich at The Ohio State University and Dr. Marc Simard at the University of Maryland. The original *Aims* are highlighted.

Aim 1: Compare patterns of acute post-hemorrhagic necrosis, delayed secondary neurodegeneration and chronic functional recovery after varying the location and magnitude of a spinal contusion injury.

At Ohio State, serial T2-weighted MRI images were collected at 6 and 24 hours post-injury in rats subject to a spinal contusion injury. Both the severity and location of injury were changed to create six different experimental groups: (1) Midline (M) severe (50 mm); (2) M moderate (25 mm); (3) M light (12.5 mm); (4) Lateral (L) severe (50 mm); (5) L moderate (25 mm) and (6) L light (12.5 mm). Data in Figs. 1-4 show how varying injury severity and location influence the magnitude and progression of secondary hemorrhage.

Regardless of the location or severity of injury, intraspinal hemorrhage increases significantly between 6 and 24 hours post-injury (**Fig. 1**). However, the volume of intraspinal hemorrhage at 6h (i.e., primary hemorrhage) was not predictive of injury severity or injury location (**Fig. 2**).

By 24 hours there was a trend for hemorrhage volume to increase as a function of injury severity, especially when the impact was directed at the spinal cord midline (**Fig. 2**). Thus, when used alone, routine measurement of intraspinal hemorrhage volume at 6 or 24 hours after SCI, does not seem to be a useful prognostic indicator of glibenclamide efficacy.

Because intraspinal hemorrhage is evident within 15 minutes of SCI (**Fig. 3**), it is possible that by 6h, primary hemorrhage has already started to transition into secondary hemorrhage. If this is true, then the optimal window for detecting a radiological signature that is predictive of glibenclamide efficacy may <6h. We next tested whether different models of injury severity and injury location produce distinct patterns and kinetics of secondary hemorrhage. Accordingly, the hemorrhage volume was calculated both

ipsilateral and contralateral to the site of injury 6 and 24 hours post-injury in the same

animals. Before-after plots (**Fig. 4**) show that

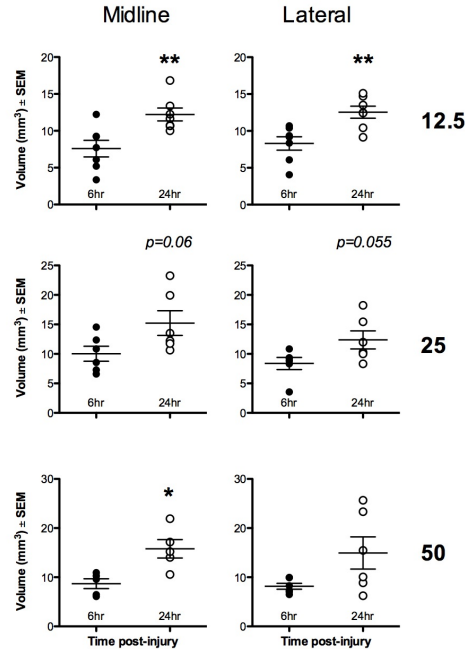


Fig 1. Intraparenchymal hemorrhage volume as a function of injury severity and location. Each data point represents a single measurement from serial T2-weighted MRI images for a single animal at 6 and 24h (n=5-7 rats/time/group; *, ** = p < 0.05 or p < 0.01, respectively vs. 6h).

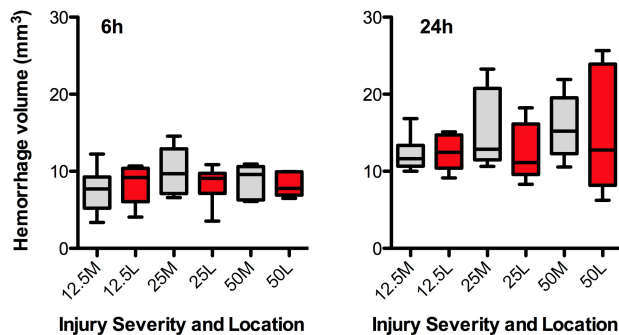


Fig 2. Box and whisker plots of data from Fig. 1 illustrating mean differences (and variability) in hemorrhage as a function of injury severity and location.

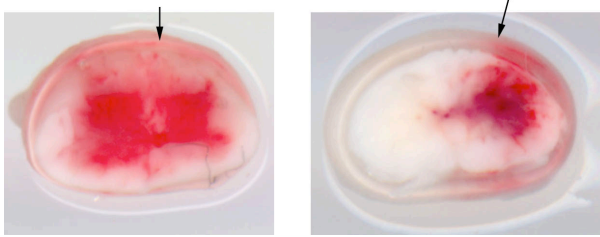


Fig 3. Injured cervical spinal cord sections 15 min post-injury. Arrows signify the angle and location of impact. Note the restricted distribution of blood in the spinal cord ipsilateral to the injury when the injury is lateral (right image). In contrast, bilateral primary hemorrhage is evident with a vertically oriented impact located near the midline (left image).

secondary hemorrhage continues to progress between 6 and 24 hours post-injury but this progression of PHN is more easily observed in spinal cords subjected to “lateralized” hemicord injury. Flat connecting lines between ipsilateral and contralateral data points indicate no difference in the percent change in hemorrhage at 24h relative to measurements at 6h. A positive slope (increase in the contralateral cord relative to ipsilateral) indicates significant spread of hemorrhage to the “uninjured” cord by 24h. With few exceptions, there is limited spread of secondary hemorrhage (PHN) after midline SCI, presumably because the location of injury causes bilateral primary hemorrhage within 6h. If so, the therapeutic window and perhaps the relative efficacy of Glib will vary as a function of injury location and severity.

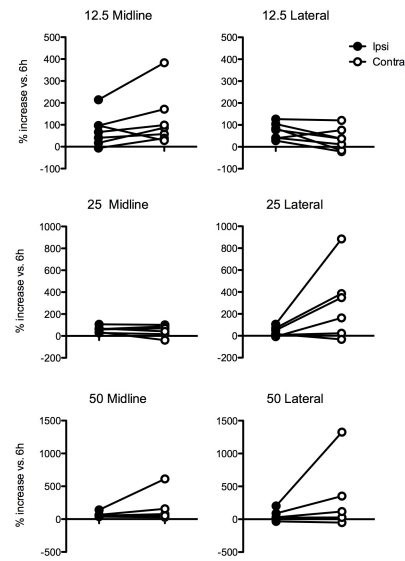


Fig 4. Before-after plots illustrating the magnitude of change in the spread of intraspinal hemorrhage at 24h (relative to the same side at 6h).

We tested this latter hypothesis directly. Specifically, we studied the effect of Glib in 2 rat cervical hemicord contusion models with identical impact force (10g, 25 mm), one with the impactor positioned laterally to yield unilateral primary hemorrhage (UPH), and the other with the impactor positioned medially, yielding larger, bilateral primary hemorrhages (BPH) that were 45% larger (Fig. 5). Functional outcome measures included: modified (unilateral) Basso, Beattie, and Bresnahan open-field locomotor scores, angled plane performance, and rearing times. In the UPH model, the effects of glibenclamide were similar to previous observations, including a functional benefit as early as 24 h post-injury and 6-week lesion volumes that were 57% smaller than controls. In the BPH model, glibenclamide exerted a significant benefit over controls, but the functional benefit was smaller than in the UPH model and 6-week lesion volumes were 33% smaller than controls (Figs. 6&7). We conclude that glibenclamide is beneficial in different models of cervical SCI, with the magnitude of the benefit depending on the magnitude and extent of primary

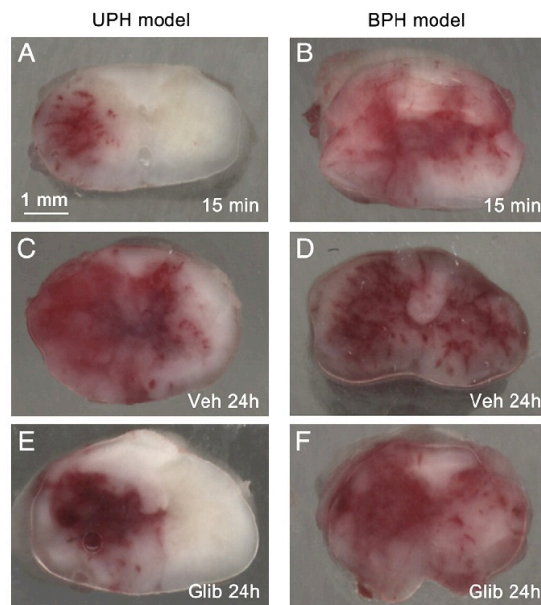


Fig 5. Patterns of primary and secondary hemorrhage and effect of glibenclamide. (A)–(F) Representative coronal sections of perfusion-cleared but otherwise unprocessed spinal cords through the epicenter of injury 15 min (A,B) and 24 h (C–F) after impact, in vehicle-treated rats from the UPH (C) and BPH (D) models, and in glibenclamide-treated rats from the UPH (E) and BPH (F) models. N=4 rats/group. (from Simard et al., 2012).

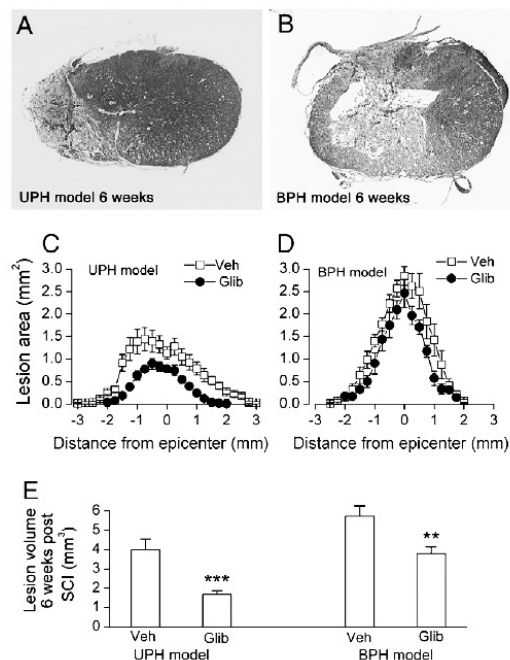


Fig 7. Effect of glibenclamide on lesion volumes. (A,B) Representative H&E-stained sections from the epicenter in vehicle-treated rats from the UPH (A) and BPH (B) models. (C,D) Lesion areas as a function of distance from the epicenter in vehicle-treated (empty squares) and glibenclamide-treated (filled circles) rats from the UPH (C) and BPH (D) models. (E,F) Lesion volumes in vehicle-treated and glibenclamide-treated rats from the UPH (E) and BPH (F) models; 8–9 rats per group; **, P<0.01; ***, P<0.001. (from Simard et al., 2012).

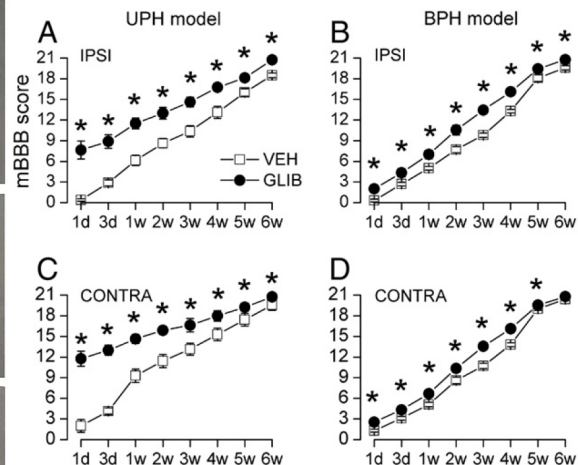


Fig 6. Effect of glibenclamide on mBBB scores. (A)–(D) Serial measurements of mBBB scores for the ipsilateral hindlimb (A,B) and for the contralateral hindlimb (C,D) in vehicle-treated (empty squares) and glibenclamide-treated (filled circles) rats from the UPH (A,C) and BPH (B,D) models; 8–9 rats per group; data are shown as mean \pm S.E.; statistical significance was determined using the Conover method; *, P<0.05; the abscissa gives time in days (d) or weeks (w). (from Simard et al., 2012).

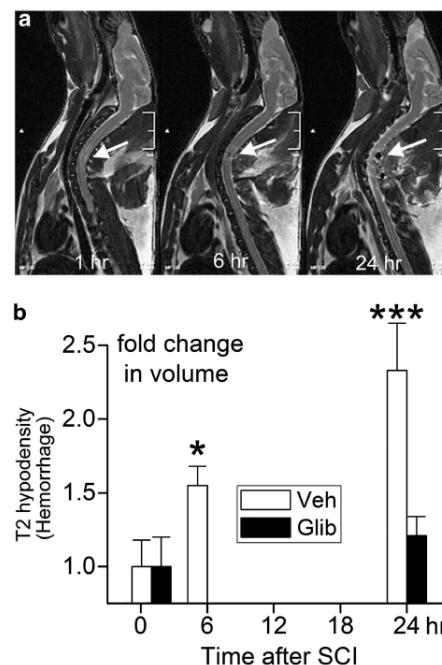


Fig 8. Progressive expansion of hemorrhagic contusion assessed using MRI. (a) Serial MRIs of a control rat obtained at 1, 6 and 24h after trauma, showing progressive enlargement of the T2 hyperdensity due to the presence of increasing amount of hemoglobin; the data shown are representative of six rats. (b) Fold-change in volumes of T2 hyperdensity measured at the times indicated in control rats (Veh; empty bars) versus glibenclamide treated rats (Glib; filled bars); mean \pm S.E.; six rats per group; *P<0.05; ***P<0.001. (from Simard et al., 2013).

We next tested whether magnetic resonance imaging (MRI) (as described above for Figs. 1-4) could be used as a non-invasive biomarker capable of revealing the efficacy of glibenclamide, especially in the acute post-injury setting. Our published data show that hemorrhagic contusion lesions expanded 2.3 ± 0.33 -fold ($P < 0.001$) during the first 24h post-SCI. Lesion expansion was reduced by $\sim 50\%$ (1.2 ± 0.07 -fold) in glibenclamide-treated rats (Fig. 8).

Recent preclinical studies have identified three treatments that are especially promising for reducing acute lesion expansion after SCI: riluzole, systemic hypothermia, and glibenclamide. Using the cervical hemicord contusion model described above (UPH), we compared safety and efficacy measures for the three treatments, administered beginning 4 hours after SCI. Treatment-associated mortality was 30% (3/10), 30% (3/10), 12.5% (1/8) and 0% (0/7), in control, riluzole, hypothermia and glibenclamide groups, respectively. For survivors, all three treatments showed overall favorable efficacy compared to controls. On open field locomotor scores (modified Basso, Beattie and Bresnahan scores), hypothermia- and glibenclamide-treated animals were largely indistinguishable throughout the study, whereas riluzole-treated rats underperformed for the first 2 weeks; during the last 4 weeks, scores for the three treatments were similar, and significantly different from controls. On beam balance, hypothermia and glibenclamide treatments showed significant advantages over riluzole. After trauma, rats in the glibenclamide group rapidly regained a normal pattern of weight gain that differed markedly and significantly from that in all other groups. Lesion volumes at 6 weeks were: 4.8 ± 0.7 , 3.5 ± 0.4 , 3.1 ± 0.3 and 2.5 ± 0.3 mm³ in the control, riluzole, hypothermia and glibenclamide groups, respectively (Fig. 9). Overall, in terms of safety and efficacy, systemic hypothermia and glibenclamide were superior to riluzole.

Aim 2: In humans with SCI, we will analyze MRI abnormalities (intraspinal edema and hemorrhage) and serum biomarkers obtained within 8 h of SCI in the same patients. Serum biomarker panels also will be correlated with ASIA motor scores at 6 months.

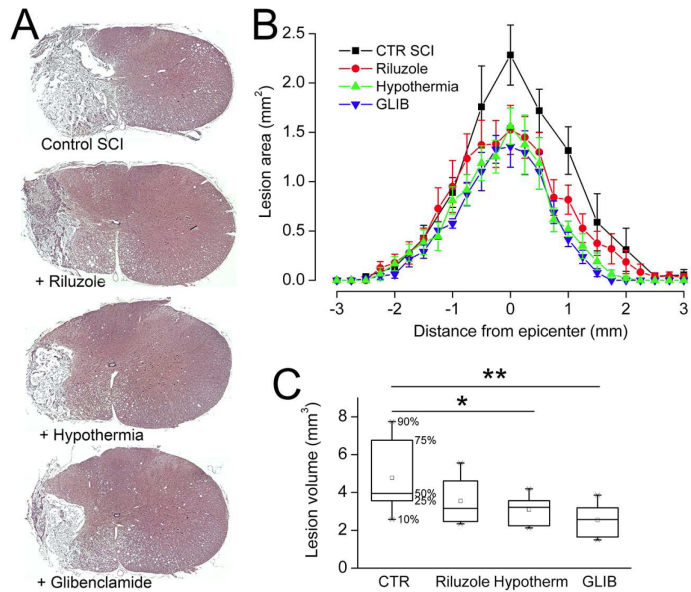


Fig. 9. At the end of the 6-week period of testing, the rats were euthanized and the spinal cords were processed to measure lesion volumes. Lesion areas were measured on serial H&E sections (Fig. 9A,B) and were used to calculate lesion volumes (Fig. 9C). Lesion volumes were: 4.8 ± 0.7 , 3.5 ± 0.4 , 3.1 ± 0.3 and 2.5 ± 0.3 mm³ in the control, riluzole, hypothermia and glibenclamide groups, respectively. N=7/grp. (submitted)

We have collected MRI data and sera from n=17 SCI patients. At the conclusion of funding from this report, data analyses for the serum/radiological biomarker correlations have not been completed. Serum samples have been collected from all rats shown in Figs. 1-4.

KEY RESEARCH ACCOMPLISHMENTS:

- Established sequential high-field T1 and T2 weighted MRI imaging protocols in rat model of SCI.
- Established that glibenclamide is neuroprotective across different types of SCI but that efficacy is related to the location/magnitude of primary hemorrhage.
- Established that non-invasive MRI (T2) imaging can predict glibenclamide efficacy within 24h post-SCI.
- Compared the relative efficacy of glibenclamide with other neuroprotective drugs (Riluzole, systemic hypothermia). Data show that glibenclamide has superior neuroprotective effects.
- Collected sera from rodents and humans with SCI for future biomarker analysis

REPORTABLE OUTCOMES:

- Disclosed above.

REFERENCES:

[Spinal cord injury with unilateral versus bilateral primary hemorrhage--effects of glibenclamide.](#) **Simard JM, Popovich PG, Tsymbalyuk O, Gerzanich V.** Exp Neurol. 2012 Feb;233(2):829-35. doi: 10.1016/j.expneurol.2011.11.048. Epub 2011 Dec 14. PMID: 22197047

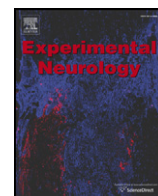
[MRI evidence that glibenclamide reduces acute lesion expansion in a rat model of spinal cord injury.](#) **Simard JM, Popovich PG, Tsymbalyuk O, Caridi J, Gullapalli RP, Kilbourne MJ, Gerzanich V.** Spinal Cord. 2013 Nov;51(11):823-7. doi: 10.1038/sc.2013.99. Epub 2013 Sep 17. PMID: 24042989

APPENDICES:

- Above referenced manuscripts

SUPPORTING DATA:

- Data are embedded in body of text above.



Spinal cord injury with unilateral versus bilateral primary hemorrhage — Effects of glibenclamide

J. Marc Simard^{a,b,c,*}, Phillip G. Popovich^d, Orest Tsybalyuk^a, Volodymyr Gerzanich^a

^a Department of Neurosurgery, University of Maryland School of Medicine, Baltimore, MD 21201, USA

^b Department of Pathology, University of Maryland School of Medicine, Baltimore, MD 21201, USA

^c Department of Physiology, University of Maryland School of Medicine, Baltimore, MD 21201, USA

^d Center for Brain and Spinal Cord Repair and Department of Neuroscience, The Ohio State University College of Medicine, Columbus, OH 43210, USA

ARTICLE INFO

Article history:

Received 6 June 2011

Revised 12 October 2011

Accepted 29 November 2011

Available online 14 December 2011

Keywords:

Spinal cord injury

Hemorrhage

Glibenclamide

ABSTRACT

In spinal cord injury (SCI), block of Sur1-regulated NC_{Ca}-ATP channels by glibenclamide protects penumbral capillaries from delayed fragmentation, resulting in reduced secondary hemorrhage, smaller lesions and better neurological function. All published experiments demonstrating a beneficial effect of glibenclamide in rat models of SCI have used a cervical hemicord impact calibrated to produce primary hemorrhage located exclusively ipsilateral to the site of impact. Here, we tested the hypothesis that glibenclamide also would be protective in a model with more extensive, bilateral primary hemorrhage. We studied the effect of glibenclamide in 2 rat cervical hemicord contusion models with identical impact force (10 g, 25 mm), one with the impactor positioned laterally to yield unilateral primary hemorrhage (UPH), and the other with the impactor positioned more medially, yielding larger, bilateral primary hemorrhages (BPH) and 6-week lesion volumes that were 45% larger. Functional outcome measures included: modified (unilateral) Basso, Beattie, and Bresnahan scores, angled plane performance, and rearing times. In the UPH model, the effects of glibenclamide were similar to previous observations, including a functional benefit as early as 24 h after injury and 6-week lesion volumes that were 57% smaller than controls. In the BPH model, glibenclamide exerted a significant benefit over controls, but the functional benefit was smaller than in the UPH model and 6-week lesion volumes were 33% smaller than controls. We conclude that glibenclamide is beneficial in different models of cervical SCI, with the magnitude of the benefit depending on the magnitude and extent of primary hemorrhage.

© 2011 Elsevier Inc. All rights reserved.

Introduction

In spinal cord injury (SCI), inhibition of Sur1-regulated NC_{Ca}-ATP channels by gene suppression in *Abcc8*−/− mice or by antisense oligodeoxynucleotide directed against *Abcc8* mRNA, as well as pharmacological blockade of Sur1 using glibenclamide or repaglinide, protects penumbral capillaries from delayed fragmentation (Simard et al., 2007; Simard et al., 2010). As a result, the formation of secondary petechial hemorrhages in the penumbra is prevented, the total amount of hemorrhage that accumulates during the first 12 h after impact is halved, lesion volumes measured at 1 and 6 weeks are reduced 2–3-fold, and various measures of neurological function assessed out to 6 weeks are significantly improved compared to controls (Simard et al., 2007; Simard et al., 2010). Independent replication of some of these findings has been reported (Popovich et al., 2011).

To date, published experiments demonstrating a beneficial effect of glibenclamide after SCI in rats have used a cervical hemicord impact in which care was taken to obtain a primary hemorrhage exclusively ipsilateral to the site of impact. This model was used because it emphasizes the distinction between primary and secondary hemorrhage, and it shows the influence of secondary hemorrhage on outcome (Simard et al., 2010). When primary hemorrhage is located exclusively unilaterally, subsequent spread of the hemorrhagic lesion to the contralateral side during the ensuing hours – by definition, secondary hemorrhage – is readily discerned both histologically and functionally. Moreover, if primary hemorrhage is confined to one side and if secondary expansion of the hemorrhagic lesion to the contralateral side is prevented, the magnitude and importance of secondary hemorrhage is readily appreciated.

Many spinal cord injuries, both clinical and experimental, involve bilateral primary injury that yields bilateral primary hemorrhage. Neurological dysfunction due to secondary hemorrhage is more difficult to detect with bilateral compared to unilateral primary injury. When the primary hemorrhage already occupies most of a spinal segment, expansion laterally of secondary hemorrhage may be limited or mute. Rostro-caudal expansion would still occur but,

* Corresponding author at: Department of Neurosurgery, 22 S. Greene St., Suite S12D, Baltimore, MD 21201-1595, USA. Fax: +1 410 328 0124.

E-mail address: msimard@smail.umaryland.edu (J.M. Simard).

depending on the spinal cord level involved, this may be difficult to detect neurologically.

The question arose whether glibenclamide would have a beneficial effect in an injury model characterized by bilateral primary hemorrhage. Here, we examined this question by studying the effect of glibenclamide in two rat cervical hemicord impact models: in the first model, the impact force and location were identical to those previously described, which results exclusively in unilateral primary hemorrhage (UPH); in the second model, the same impact force was applied more medially, resulting in bilateral primary hemorrhage (BPH) and lesion volumes at 6 weeks that were 45% larger than in the UPH model. In brief, the effects of glibenclamide in the UPH model were similar to previous observations, including a significant neurological benefit that was apparent as early as 24 h after injury, and lesion volumes at 6 weeks that were 57% smaller than in controls. In the BPH model, glibenclamide was beneficial, but the neurological benefit and the reduction in lesion volume (33% smaller than in controls) were less than in the UPH model.

Methods

Subjects and experimental series

All experimental procedures were approved by the University of Maryland Institutional Animal Care and Use Committee. In accordance with “good laboratory practice”, different investigators blinded to injury-group conducted behavioral tests and analyses of data.

Fifty-eight female Long–Evans rats (250–300 g; Harlan, Indianapolis, IN) were used in 2 experimental series, the first to determine the pattern of primary and secondary hemorrhage in each model, and the second to study the effect of glibenclamide in each model. In series 1, 24 rats underwent SCI (see below), 12 with the impact delivered “laterally” (UPH model), and 12 with the impact delivered “medially” (BPH model). For rats in each impact group, 4 were euthanized at 15 min, 4 were administered vehicle, 4 were administered glibenclamide (see below) and the 8 rats were euthanized at 24 h. In series 2, 34 rats underwent SCI, 16 with the UPH model and 18 with the BPH model. For rats in each group, half received vehicle and half received glibenclamide. Rats in this series were maintained for 6 weeks after injury, during which they underwent serial measurements of locomotor function, and after which they were euthanized to measure lesion volumes.

Rat models of SCI

We used two rat models of unilateral cervical SCI that were slightly modified from the original description (Soblosky et al., 2001), one of which (the UPH model) was reported by us previously (Simard et al., 2007; Simard et al., 2010).

Female Long–Evans rats (~11 weeks; 250–300 g; Harlan) were anesthetized (Ketamine, 60 mg/kg plus Xylazine, 7.5 mg/kg, IP) and the head was mounted in a stereotaxic apparatus (Stoelting, Wood Dale, IL). Using aseptic technique and magnification (Zeiss operating microscope with co-axial lighting), the spine was exposed dorsally from C3 to T3 via a 3-cm midline incision and subperiosteal dissection of the paraspinal muscles. The ear bars were removed and the animal was repositioned so that it was supported from the spinous process of T2 (Spinal Adaptor, Stoelting) and the snout. On the left side, the entire lamina of C7 and the dorsal half of the pedicle of C7 were removed using a 1.9-mm diamond burr (#HP801-019, DiamondBurs.Net) and a high-speed drill, with care taken to avoid mechanical and thermal injury to the underlying dura and spinal cord. For the UPH model, a unilateral laminectomy was used as described whereas, for the BPH model, the laminectomy was extended to include the contralateral side. The dura was exposed by sharply removing the interlaminar ligaments rostral and caudal to the lamina of C7

and any remaining ligamentum flavum. The guide tube was angled 5° medially and was positioned using the manipulator arm of the stereotaxic apparatus. The impactor (1.55-mm tip diameter, 57 mm length, 1.01 g) (Soblosky et al., 2001) was gently lowered down the guide tube and was positioned on the dura at the desired location. The impactor was then activated when struck by a 10 g weight released from a height of 25 mm inside the guide tube (velocity, 0.7 m/s).

For both models, the impactor was carefully positioned on the dura mater near the left C8 nerve root, with the caudal edge of the impactor in line with the caudal edge of the C8 nerve root at the axilla (Fig. 1). For the UPH model, the medial edge of the impactor was positioned 0.3 mm medial to the dorsolateral sulcus, as previously (Simard et al., 2007; Simard et al., 2010). For the BPH model, the lateral edge of the impactor was positioned 0.3 mm lateral to the dorsolateral sulcus, which placed the medial edge of the impactor at the midline. With the UPH model, the impact caused an immediate, forceful flexion of the trunk and 70–90° flexion of the ipsilateral knee, which had been extended before impact. With the BPH model, flexion of the trunk and of the ipsilateral knee was less pronounced.

After injury, the surgical site was flushed with 1 ml of normal saline (NS), the musculature was replaced over the spine and the skin incision was stapled. Within 5–10 min of injury, all rats were administered a “treatment”, either vehicle or glibenclamide (see below). Rats were nursed on a heating pad to maintain rectal temperature ~37 °C, and were given 10 ml of glucose-free NS subcutaneously. Food and water were placed within easy reach to ensure that the rats were able to eat and drink without assistance. Bladder function was assessed 2–3 times daily by observing for urination and, if needed, manual emptying of the bladder was carried out using the Credé maneuver.

Treatments

Treatment consisted of administering a loading dose IP plus implanting a mini-osmotic pump for continuous 1-week long subcutaneous delivery of either vehicle or glibenclamide. A fresh stock solution of glibenclamide, different from the stock solutions previously used (Simard et al., 2007; Simard et al., 2010; Popovich et al., 2011), was prepared by placing 25 mg glibenclamide (#G2539; meets USP testing; Sigma, St. Louis, MO) into 10 ml dimethyl sulfoxide (DMSO). The solution to be loaded into the mini-osmotic pumps (Alzet 2001, 1.0 µl/h; Alzet Corp., Cupertino, CA) was made by taking 2.3 ml unbuffered NS, adding 4 µl of 10 N NaOH, then adding 200 µl stock solution, in that order to prevent precipitation of drug. The solution to be used for the loading dose was made by adding 4 µl of stock solution to 1 ml NS. For vehicle controls, solutions were made with DMSO and NS as above, but glibenclamide was omitted.

After loading, the mini-osmotic pumps were primed overnight in NS at 37 °C with the outlet of the pump connected to a length of PE-60 tubing that extended above the level of the priming solution, to prevent H⁺ ions from entering the pump chamber.

Loaded and primed mini-osmotic pumps were implanted subcutaneously after completing surgery to induce SCI; pumps containing drug delivered 200 ng/h of glibenclamide for 7 days. A few minutes after surgery, the loading dose was administered IP, with the volume of the loading dose in microliters equal to the weight of the rat in grams (syringes with glibenclamide delivered 10 µg/kg IP). Infusion of 200 ng/h of glibenclamide yields plasma concentrations ~5 ng/ml (Simard, unpublished observation) and has a minimal effect on serum glucose (Simard et al., 2006; Simard et al., 2007; Simard et al., 2009).

Treatment coding and allocation

The syringes and mini-osmotic pumps used to deliver the “treatments” were prepared by one investigator, after which they were

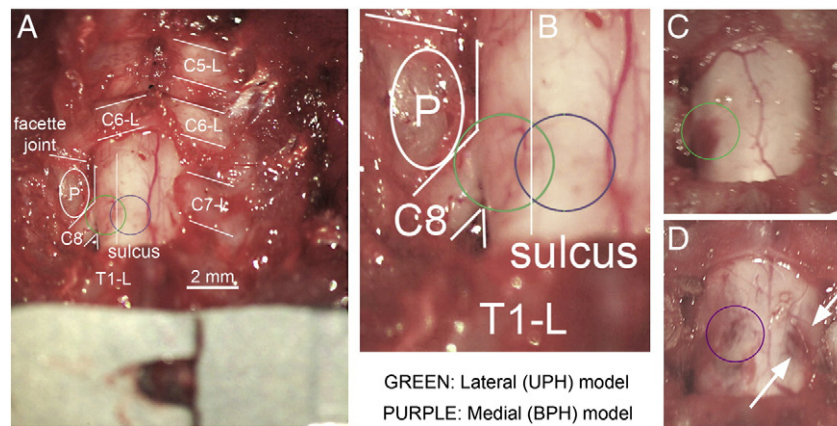


Fig. 1. Impact locations and initial contusions for the UPH and BPH models. (A,B) Low (A) and high (B) magnification photomicrographs of the surgical exposure used for cervical hemicord contusion injury; after removing the spinous processes from C5 to T1, the entire left and part of the right lamina of C7 and the interlaminar ligaments and ligamentum flavum at C7, the left hemicord at C7 is visualized through the translucent dura; the anatomical details visualized include the laminae (L) of cervical (C) and thoracic (T) vertebral levels C5 through T1, the left facet joint between C6 and C7, the C8 nerve root exiting the spinal canal caudal to the left pedicle (P) of C7, and the dorsolateral sulcus of the spinal cord, from which emerges the rootlets of the dorsal roots; note the metallic clamp on the spinous process of T2 in (A); the 1.55 mm diameter impactor used to produce contusion injury is directed at an angle of 5° medially and is positioned to strike the spinal cord in the area denoted by the green or purple circles for the UPH and BPH models, respectively; adapted from Simard et al., 2010. (C,D) Intraoperative photomicrographs showing contusions on the surface of the spinal cord evident 2 min after impact, for the UPH model (C) and for the BPH model (D); the contralateral hemorrhage evident at the surface in the BPH model is indicated by arrows.

coded by a separate investigator so that the surgeon performing the SCI and administering the treatment was unaware of their content ("blinded").

Treatment allocation was determined daily by the same investigator who coded the syringes and pumps, but who otherwise did not participate in the experiment. On each day, 4 treatment sets were prepared, each consisting of a syringe with the loading dose and a mini-osmotic pump with the infusion solution; 2 sets contained vehicle and 2 sets contained glibenclamide. The order for administering vehicle or glibenclamide in 4 successive rats with SCI was determined by coin toss.

Measurements of primary and secondary hemorrhage

At the designated time after injury (15 min for primary hemorrhage; 24 h for primary plus secondary hemorrhage), the rat was anesthetized with sodium pentobarbital (100 mg/kg), a thoracotomy was performed, and the rat was transcardially perfused with NS (50 ml) at a pressure of 100 cm H₂O. The spinal cord was harvested, sectioned coronally through the epicenter of injury, and the face of the epicenter was imaged at high resolution using a flat-bed scanner.

Locomotor function

Basso, Beattie and Bresnahan (BBB) scores were determined as described (Basso et al., 1995), except that modifications were introduced to allow more accurate assessment of the functional asymmetry associated with hemicord injury. The scoring sheet shown in Fig. 1 of the original paper (Basso et al., 1995) provides for scoring of the right and left hindlimbs separately, with the final score for the animal being based on the two scores. Here, because we were studying hemicord injuries, we maintained the two scores separately, which we refer to as modified BBB (mBBB) scores. The method for scoring up to and including scores of 11 is identical for mBBB and BBB. For mBBB scoring of coordination, forelimb–hindlimb coordination was operationally defined as a one-to-one correspondence between forelimb and *ipsilateral* hindlimb steps on each side; "alternation in hindlimb stepping", which is taken into account in BBB scoring, was ignored for mBBB scoring. For scores above 19,

both right and left sides were credited for "tail consistently up" and for "trunk stability".

Tests to determine the angle of failure on up-angled and down-angled planes (Rivlin and Tator, 1977) were performed on a wooden surface (unfinished Luan plywood) with the plane position raised from horizontal at ~5°/s. The better of two consecutive tests was taken as the final measure.

To measure rearing times, rats were videotaped while in a translucent cylinder (19 × 20 cm) and spontaneous rearing was quantified as the number of seconds spent with both front paws elevated above shoulder-height during a 3-minute period of observation (Simard et al., 2007). In separate experiments, assessment of rearing behavior in sham-lesioned rats showed that performance waned after 2–3 weeks, presumably because the rats became habituated to the test chamber.

Lesion volume

At 6 weeks after SCI, the rats were deeply anesthetized, perfusion-fixed with 10% neutral buffered formalin, and the spinal cords were harvested. Serial paraffin sections were stained with hematoxylin and eosin (H&E). Lesion areas (in mm²) were measured on serial sections every 250 μm; lesion volumes (in mm³) were calculated as the sum of the areas multiplied by 0.25.

Data analysis

Like BBB scores (Scheff et al., 2002; Ferguson et al., 2004; Barros Filho and Molina, 2008), mBBB scores are derived from an ordinal scale and are not normally distributed. Therefore, we analyzed mBBB scores using a nonparametric (distribution-free) procedure based on ranks (Conover and Iman, 1981). mBBB scores were rank-transformed as described (Conover and Iman, 1981) prior to the application of parametric statistical analysis. Rearing times (Kilbourne et al., 2009) and angled plane performance are normally distributed. Serial measurements of the ranks of mBBB scores, the angles, and the rearing times were analyzed using a 2-way mixed-model repeated measures ANOVA, with Tukey post-hoc comparisons. Lesion volumes were analyzed using an ANOVA.

Results

Ipsilateral vs. bilateral primary hemorrhage models

We studied the effect of an impact force (10 g, 25 mm, 0.7 m/s) applied to the left lower cervical hemicord, delivered in two different locations, one with the impact directed “laterally”, as used previously in this laboratory, and the other with the impact directed “medially” (see [Methods](#)).

Initial contusion

The initial contusion produced by the impact was observed as it developed within 1–2 min of impact, visualizing it through the intact, translucent dura under the operating microscope.

With the “lateral” impact, a hemorrhagic contusion was evident that involved the lateral surface of the cord extending up to the dorsolateral sulcus, but not more medially and never contralaterally ([Fig. 1C](#)).

With the “medial” impact, a hemorrhagic contusion was evident that approximated the size and shape of the impactor on the ipsilateral dorsal surface of the cord, and that had rostral and caudal expansion of bleeding evident within the ipsilateral sulcus, and also had a short strip of hemorrhage evident within the contralateral sulcus ([Fig. 1D](#)).

Primary hemorrhage at 15 min

The hemorrhage present within the spinal cord 15 min after impact was considered to be the primary hemorrhage. The primary hemorrhage was assessed by imaging a coronal section of the spinal cord through the epicenter that was prepared after removing intravascular contents by perfusion.

With the “lateral” impact, the primary hemorrhage was limited to the ipsilateral cord, including the dorsolateral funiculus and dorsal horn, with variable extension into the ventral horn ([Fig. 2A](#)).

Subsequent experiments that utilized the “lateral” impact site are designated as the unilateral primary hemorrhage (UPH) model.

With the “medial” impact, the primary hemorrhage was invariably located both ipsilaterally and contralaterally in gray matter and white matter ([Fig. 2B](#)). Subsequent experiments that utilized the “medial” impact site are designated as the bilateral primary hemorrhage (BPH) model.

Effects of glibenclamide

Primary plus secondary hemorrhage at 24 h

After SCI, progressive hemorrhagic necrosis continues to expand the hemorrhagic lesion for ~12 h after impact, after which it reaches steady-state ([Zhang et al., 1996; Guth et al., 1999; Simard et al., 2007](#)). Thus, the hemorrhage present 24 h after impact was considered to consist of both primary plus secondary hemorrhage. The primary plus secondary hemorrhage was assessed by imaging a coronal section of the spinal cord through the epicenter that was prepared after removing intravascular contents by perfusion.

With the UPH model in vehicle treated rats, hemorrhage at 24 h typically extended through much of the ipsilateral cord and well into the contralateral gray and white matter ([Fig. 2C](#)), representing significant progression compared to the primary hemorrhage evident at 15 min ([Fig. 2A](#)). In glibenclamide-treated rats, there was no progression of hemorrhage at 24 h compared to 15 min; the hemorrhage was confined to the ipsilateral spinal cord ([Fig. 2E](#)). These observations are consistent with glibenclamide halting progressive hemorrhagic necrosis ([Simard et al., 2007; Simard et al., 2010](#)).

With the BPH model in vehicle treated rats, hemorrhage at 24 h typically extended through much of the ipsilateral cord and well into the contralateral gray and white matter ([Fig. 2D](#)), similar to observations at 15 min. In glibenclamide-treated rats, hemorrhage at 24 h was located bilaterally, with the pattern of hemorrhage largely indistinguishable from vehicle-treated rats ([Fig. 2F](#)). The apparent absence of an effect of glibenclamide was attributed to the presence of bilateral primary hemorrhage in this model that precluded or masked any potential reduction in contralateral spread of hemorrhage.

Locomotor function

mBBB scores for each hindlimb, performance on an angled plane, and spontaneous rearing were measured serially over the course of 6 weeks in rats from both the UPH and the BPH models that were administered either vehicle or glibenclamide.

With the UPH model, glibenclamide-treated rats fared significantly better than vehicle-treated rats in both ipsilateral and contralateral lower extremity function ([Figs. 3A,B](#)). mBBB scores contralateral to the injury were highly different 24 h after injury in glibenclamide-treated rats compared to vehicle-treated rats. Scores were consistently better with glibenclamide but, by 6 weeks, vehicle-treated rats had recovered contralateral function almost to the level of the glibenclamide-treated rats. mBBB scores ipsilateral to the injury also were highly different 24 h after injury in glibenclamide-treated rats compared to vehicle-treated rats, with ipsilateral mBBB scores showing persistent discrimination throughout the 6 weeks of testing.

With the BPH model, glibenclamide-treated rats also fared significantly better than vehicle-treated rats in both ipsilateral and contralateral lower extremity function, but the treatment effect was smaller ([Figs. 3C,D](#)). mBBB scores contralateral to the injury were similar 24 h after injury in glibenclamide-treated rats compared to vehicle-treated rats. Scores were consistently better with glibenclamide, but by 6 weeks vehicle-treated rats had recovered contralateral function to the level of the glibenclamide-treated rats. mBBB scores ipsilateral to the injury showed persistent discrimination throughout the 6 weeks of testing.

The ability to maintain position on an angled plane is a complex task that assesses the coordinated function of all 4 limbs and is therefore an excellent test of cervical spinal cord function. With both the UPH and

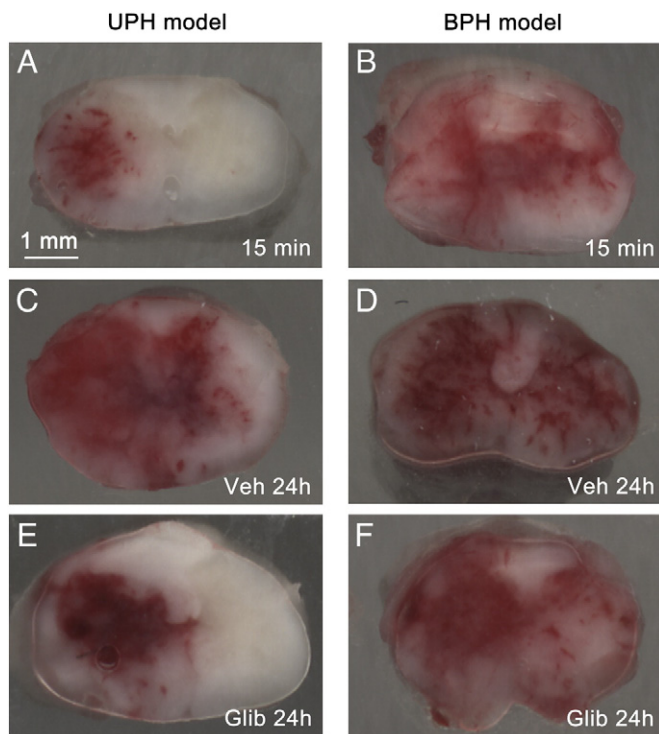


Fig. 2. Patterns of primary and secondary hemorrhage and effect of glibenclamide. (A)–(F) Representative coronal sections of perfusion-cleared but otherwise unprocessed spinal cords through the epicenter of injury 15 min (A,B) and 24 h (C–F) after impact, in vehicle-treated rats from the UPH (C) and BPH (D) models, and in glibenclamide-treated rats from the UPH (E) and BPH (F) models. The data shown are representative of 4 rats per group.

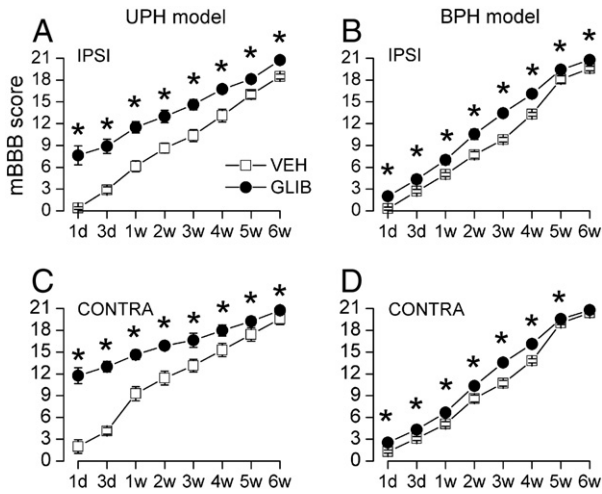


Fig. 3. Effect of glibenclamide on mBBB scores. (A)–(D) Serial measurements of mBBB scores for the ipsilateral hindlimb (A,B) and for the contralateral hindlimb (C,D) in vehicle-treated (empty squares) and glibenclamide-treated (filled circles) rats from the UPH (A,C) and BPH (B,D) models; 8–9 rats per group; data are shown as mean \pm S.E.; statistical significance was determined using the Conover method; *, $P<0.05$; **, $P<0.01$; the abscissa gives time in days (d) or weeks (w).

the BPH models, glibenclamide-treated rats fared significantly better than vehicle-treated rats in both the up-angled and down-angled tests (Figs. 4A,B). The effect of treatment was evident as early as 24 h after injury, and was sustained for the duration of testing.

We quantified vertical exploratory behavior (rearing), a complex exercise that requires balance, trunk stability, bilateral hind limb dexterity, and strength, and at least unilateral forelimb dexterity and strength, which together are excellent markers of cervical spinal cord function.

With the UPH model, glibenclamide-treated rats fared significantly better than vehicle-treated rats. The effect of treatment was evident as early as 24 h after injury, and was sustained for the duration of testing (Fig. 5A).

With the BPH model, glibenclamide-treated rats also fared significantly better than vehicle-treated rats. However, the effect of treatment became evident only 2 weeks after injury, after which it was sustained for the duration of testing (Fig. 5B). The performance achieved in both vehicle and glibenclamide-treated rats from the BPH model was less than that in comparable groups from the UPH model.

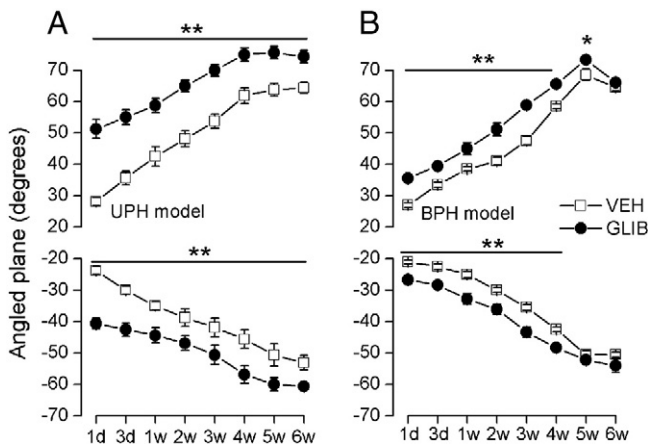


Fig. 4. Effect of glibenclamide on angled plane performance. (A,B) Serial measurements of the angle of failure (mean \pm S.E.) for up-angled and down-angled tests in vehicle-treated (empty squares) and glibenclamide-treated (filled circles) rats from the UPH (A) and BPH (B) models; 8–9 rats per group; *, $P<0.05$; **, $P<0.01$; the abscissa gives time in days (d) or weeks (w).

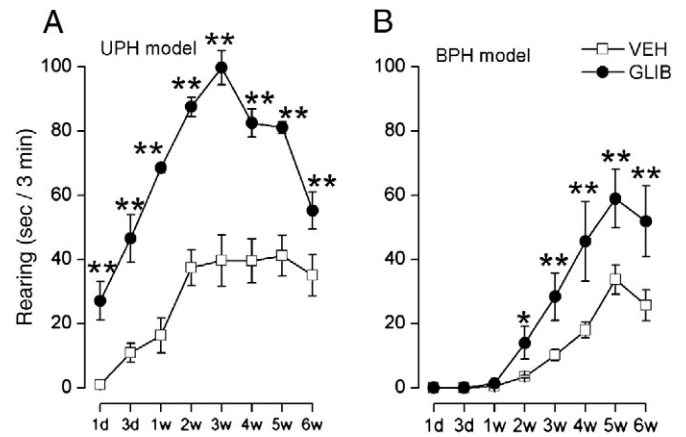


Fig. 5. Effect of glibenclamide on spontaneous rearing. (A,B) Serial measurements of the time (mean \pm S.E.) spent in spontaneous rearing in vehicle-treated (empty squares) and glibenclamide-treated (filled circles) rats from the UPH (A) and BPH (B) models; 8–9 rats per group; *, $P<0.05$; **, $P<0.01$; the abscissa gives time in days (d) or weeks (w).

Lesion volume

Lesion volumes were measured after completing the locomotor function tests at 6 weeks. In vehicle-treated rats, 6-week lesion volumes were 45% larger in the BPH model compared to the UPH model (Fig. 6). In both models, glibenclamide exerted a significant effect on tissue preservation, but the magnitude of protection was

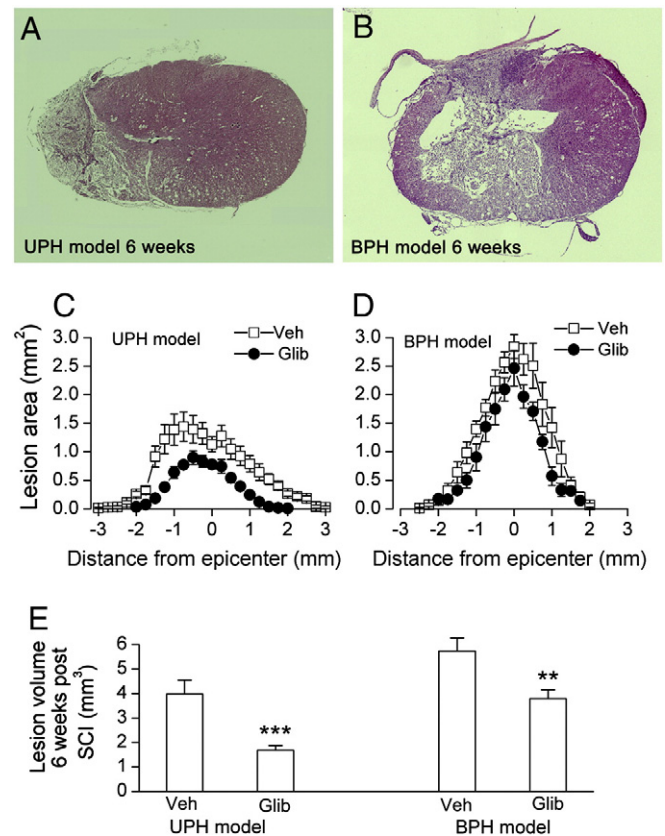


Fig. 6. Effect of glibenclamide on lesion volumes. (A,B) Representative H&E-stained sections from the epicenter in vehicle-treated rats from the UPH (A) and BPH (B) models. (C,D) Lesion areas as a function of distance from the epicenter in vehicle-treated (empty squares) and glibenclamide-treated (filled circles) rats from the UPH (C) and BPH (D) models. (E,F) Lesion volumes in vehicle-treated and glibenclamide-treated rats from the UPH (E) and BPH (F) models; 8–9 rats per group; *, $P<0.05$; **, $P<0.01$; ***, $P<0.001$.

greater with the UPH model compared to the BPH model: with the UPH model, 6-week lesion volumes with glibenclamide were 57% smaller than in controls; with the BPH model, 6-week lesion volumes with glibenclamide were 33% smaller than in controls (Fig. 6).

Discussion

The principal finding of the present study is that glibenclamide is an effective treatment for SCI, with the magnitude of the benefit depending on the magnitude of primary hemorrhagic insult. With both models, one with unilateral primary hemorrhage and the other with bilateral primary hemorrhage, glibenclamide afforded significant protection in terms of neurological function and preservation of spinal cord tissues. The effect of treatment in the UPH model was similar to our previous observations (Simard et al., 2007; Simard et al., 2010). In addition, here we show that an injury model characterized by bilateral primary hemorrhage also is influenced favorably, albeit the benefit at 6 weeks in terms of function and lesion volume was less than when the primary hemorrhagic injury was unilateral.

In SCI, the magnitude of the primary injury plays a leading role in determining outcome. Several distinct factors associated with the primary injury may be independent predictors of outcome, including physical aspects of the force generating the injury (magnitude, velocity, depth, etcetera) as well as immediate biological aspects of the response to injury (number of axons severed, amount of blood extravasated, etcetera). Among these various factors, the amount of primary hemorrhage is exceedingly important, given the role of blood in determining the magnitude of the subsequent free radical and inflammatory responses. In the models studied here, differences in apparent injury severity were not due to the magnitude of the force applied, which was identical in both cases, but were due to the specific location of the impact, which determined whether the primary hemorrhage would be unilateral or bilateral. By adjusting the location of the impact, we were able to obtain either a unilateral or a bilateral primary hemorrhage, thereby separating the biophysics of injury from the biological response to injury. In SCI research, the “severity” of a contusive injury is generally equated with impact force or tissue strain because, in any given study, the impact is typically delivered to a single location, e.g., midline, low thoracic. The data presented here suggest that, because of the anisotropy of spinal cord tissues, the same force can generate large differences in the severity of neurological injury, with severity correlating with the amount of primary hemorrhage.

SCI is normally complicated by progressive hemorrhagic necrosis, a secondary injury process that results in expansion of the hemorrhagic lesion (Balentine, 1978; Simard et al., 2007). When SCI is associated initially with a unilateral primary hemorrhage, the process of progressive hemorrhagic necrosis spreads to involve the contralateral side, resulting in a bilateral hemorrhagic lesion. Halting progressive hemorrhagic necrosis by blocking Sur1-regulated NC_{Ca-ATP} channels with glibenclamide results in hemorrhagic lesions that remain largely unilateral, significantly preserving both tissue and function (Simard et al., 2007). With an injury involving bilateral primary hemorrhage, the opportunity to reduce lesion expansion is restricted largely to rostral-caudal expansion, which yields a less dramatic benefit in terms of tissue sparing and neurological function. Notably, with the UPH model, an effect of glibenclamide was evident as early at 24 h after injury, whereas 1 week or more was required to observe a beneficial effect of glibenclamide with the BPH model. This latter observation recapitulates and expands upon a similar observation recently reported for glibenclamide (Popovich et al., 2011).

The physical properties of gray matter and white matter of the spinal cord are highly different. Compared to white matter, gray matter has 4–5 times greater capillary density (Ireland et al., 1981), is less tolerant to compression before failure of the blood–spinal cord barrier (Maikos and Shreiber, 2007), and is more fragile and ruptures at

lower strains (Ichihara et al., 2001). These features make gray matter the dominant source of primary hemorrhage following contusion injury. In addition, gray matter and white matter respond differently to injury dynamics, especially impact velocity. Whereas impact velocity has relatively little effect on the volume of primary hemorrhage in gray matter, this is not the case for white matter, where primary hemorrhage volume as well as primary axonal disruption are significantly greater with high velocity impact compared to low velocity impact (Sparrey et al., 2008).

With lower cervical cord injury, the consequences of injury to gray matter versus white matter are very different, with white matter injury having a greater impact on several aspects of neurological function. Injury (primary or secondary) to white matter interrupts ascending and descending fiber tracts, resulting in sensorimotor dysfunction below the level of injury involving trunk, lower extremities and bladder, whereas injury to gray matter results in limited segmental neuronal dysfunction which, by itself, may be tolerable. However, primary injury to gray matter results in hemorrhage, which is one of the most important triggers of secondary injury to white matter, greatly exacerbating and expanding any primary white matter injury. At present, little can be done to ameliorate primary white matter damage, but an important goal of acute treatment is to minimize secondary injury to white matter, to best preserve distal function. Because low velocity impact is less likely to produce primary white matter damage, but is still highly effective at inducing primary gray matter injury with hemorrhage (Sparrey et al., 2008), low velocity impacts may be more useful than high velocity impacts for studying secondary white matter injury and its treatment.

In SCI research, some workers have used parametric statistical methods to analyze raw BBB scores even though this approach is technically incorrect, due to the fact that BBB scores are ordinal in nature. Relying on “the robustness of ANOVA to handle violations of the normality assumption” (Scheff et al., 2002) is less than ideal, and collapsing the scale to force it to be more normal (Ferguson et al., 2004) clouds differences at the upper end of the scale. Here, we used rank transformation prior to the application of standard parametric methods (Conover and Iman, 1981). Apart from being technically appropriate, this method of analysis can yield statistically significant differences when scores are close; even if scores are no more than one point apart, consistent superiority in ranks can yield statistical significance. This approach is of clinical relevance, reflecting for example, the experience in human SCI trials on methylprednisolone where it was argued, rightly, that one additional cervical spinal level could be of great clinical importance to patients.

In summary, we report that glibenclamide is an effective treatment for spinal cord injuries associated with various amounts of primary hemorrhage. Previous work using the UPH model reported strong efficacy in two different series of rats (Simard et al., 2007; Simard et al., 2010), with the present study representing the third independent series in which a beneficial effect of glibenclamide is shown in this model. In the present study, we now show that glibenclamide treatment also favorably influences outcome in an injury model characterized by bilateral primary hemorrhage. We conclude that glibenclamide is beneficial in models of different injury severity, with the magnitude of the benefit depending on the magnitude of primary hemorrhagic insult.

Conflict of interest

JMS holds a US patent (#7,872,048), “Methods for treating spinal cord injury with a compound that inhibits a NC(Ca-ATP) channel”. JMS is a member of the scientific advisory board and holds shares in Remedy Pharmaceuticals. No support, direct or indirect, was provided to JMS, or for this project, by Remedy Pharmaceuticals.

Acknowledgment

This work was supported by grants to JMS from the Veterans Administration (Baltimore), the National Institute of Neurological Disorders and Stroke (NINDS) (NS060801), and the Christopher and Dana Reeve Foundation; to VG from NINDS (NS061934); to PGP from NINDS (HHSN271200800040C) and the Ray W. Poppleton endowment (OSU); to PGP and JMS from the Department of the Army (W81XWH 1010898).

References

- Balentine, J.D., 1978. Pathology of experimental spinal cord trauma. I. The necrotic lesion as a function of vascular injury. *Lab Invest* 39, 236–253.
- Barros Filho, T.E., Molina, A.E., 2008. Analysis of the sensitivity and reproducibility of the Basso, Beattie, Bresnahan (BBB) scale in Wistar rats. *Clinics (Sao Paulo)* 63, 103–108.
- Basso, D.M., Beattie, M.S., Bresnahan, J.C., 1995. A sensitive and reliable locomotor rating scale for open field testing in rats. *J. Neurotrauma* 12, 1–21.
- Conover, W.J., Iman, R.L., 1981. Rank transformations as a bridge between parametric and nonparametric statistics. *Am. Statistician* 35, 124–133.
- Ferguson, A.R., Hook, M.A., Garcia, G., Bresnahan, J.C., Beattie, M.S., Grau, J.W., 2004. A simple post hoc transformation that improves the metric properties of the BBB scale for rats with moderate to severe spinal cord injury. *J. Neurotrauma* 21, 1601–1613.
- Guth, L., Zhang, Z., Steward, O., 1999. The unique histopathological responses of the injured spinal cord. Implications for neuroprotective therapy. *Ann. N. Y. Acad. Sci.* 890, 366–384.
- Ichihara, K., Taguchi, T., Shimada, Y., Sakuramoto, I., Kawano, S., Kawai, S., 2001. Gray matter of the bovine cervical spinal cord is mechanically more rigid and fragile than the white matter. *J. Neurotrauma* 18, 361–367.
- Ireland, W.P., Fletcher, T.F., Bingham, C., 1981. Quantification of microvasculature in the canine spinal cord. *Anat. Rec.* 200, 102–113.
- Kilbourne, M., Kuehn, R., Tosun, C., Caridi, J., Keledjian, K., Bochicchio, G., Scalea, T., Gerzanich, V., Simard, J.M., 2009. Novel model of frontal impact closed head injury in the rat. *J. Neurotrauma* 26, 2233–2243.
- Maikos, J.T., Shreiber, D.I., 2007. Immediate damage to the blood–spinal cord barrier due to mechanical trauma. *J. Neurotrauma* 24, 492–507.
- Popovich, P.G., Limeshow, S., Gensel, J.C., Tovar, C.A., 2011. Independent evaluation of the effects of glibenclamide on reducing progressive hemorrhagic necrosis after cervical spinal cord injury. *Exp. Neurol.* (Electronic publication ahead of print).
- Rivlin, A.S., Tator, C.H., 1977. Objective clinical assessment of motor function after experimental spinal cord injury in the rat. *J. Neurosurg.* 47, 577–581.
- Scheff, S.W., Saucier, D.A., Cain, M.E., 2002. A statistical method for analyzing rating scale data: the BBB locomotor score. *J. Neurotrauma* 19, 1251–1260.
- Simard, J.M., Chen, M., Tarasov, K.V., Bhatta, S., Ivanova, S., Melnichenko, L., Tsybalyuk, N., West, G.A., Gerzanich, V., 2006. Newly expressed SUR1-regulated NC(Ca-ATP) channel mediates cerebral edema after ischemic stroke. *Nat. Med.* 12, 433–440.
- Simard, J.M., Tsybalyuk, O., Ivanov, A., Ivanova, S., Bhatta, S., Geng, Z., Woo, S.K., Gerzanich, V., 2007. Endothelial sulfonylurea receptor 1-regulated NC(Ca-ATP) channels mediate progressive hemorrhagic necrosis following spinal cord injury. *J. Clin. Invest.* 117, 2105–2113.
- Simard, J.M., Woo, S.K., Norenberg, M.D., Tosun, C., Chen, Z., Ivanova, S., Tsybalyuk, O., Bryan, J., Landsman, D., Gerzanich, V., 2010. Brief suppression of Abcc8 prevents autodestruction of spinal cord after trauma. *Sci. Transl. Med.* 2, 28ra29.
- Simard, J.M., Yurovsky, V., Tsybalyuk, N., Melnichenko, L., Ivanova, S., Gerzanich, V., 2009. Protective effect of delayed treatment with low-dose glibenclamide in three models of ischemic stroke. *Stroke* 40, 604–609.
- Soblosky, J.S., Song, J.H., Dinh, D.H., 2001. Graded unilateral cervical spinal cord injury in the rat: evaluation of forelimb recovery and histological effects. *Behav. Brain Res.* 119, 1–13.
- Sparrey, C.J., Choo, A.M., Liu, J., Tetzlaff, W., Oxland, T.R., 2008. The distribution of tissue damage in the spinal cord is influenced by the contusion velocity. *Spine (Phila Pa 1976.)* 33, E812–E819.
- Zhang, Z., Fujiki, M., Guth, L., Steward, O., 1996. Genetic influences on cellular reactions to spinal cord injury: a wound-healing response present in normal mice is impaired in mice carrying a mutation (WldS) that causes delayed Wallerian degeneration. *J. Comp. Neurol.* 371, 485–495.

ORIGINAL ARTICLE

MRI evidence that glibenclamide reduces acute lesion expansion in a rat model of spinal cord injury

JM Simard^{1,2,3}, PG Popovich⁴, O Tsybalyuk¹, J Caridi¹, RP Gullapalli⁵, MJ Kilbourne⁶ and V Gerzanich¹**Study design:** Experimental, controlled, animal study.**Objectives:** To use non-invasive magnetic resonance imaging (MRI) to corroborate invasive studies showing progressive expansion of a hemorrhagic lesion during the early hours after spinal cord trauma and to assess the effect of glibenclamide, which blocks Sur1-Trpm4 channels implicated in post-traumatic capillary fragmentation, on lesion expansion.**Setting:** Baltimore.**Methods:** Adult female Long–Evans rats underwent unilateral impact trauma to the spinal cord at C7, which produced ipsilateral but not contralateral primary hemorrhage. In series 1 (six control rats and six administered glibenclamide), hemorrhagic lesion expansion was characterized using MRI at 1 and 24 h after trauma. In series 2, hemorrhagic lesion size was characterized on coronal tissue sections at 15 min (eight rats) and at 24 h after trauma (eight control rats and eight administered glibenclamide).**Results:** MRI (T2 hypodensity) showed that lesions expanded 2.3 ± 0.33 -fold ($P < 0.001$) during the first 24 h in control rats, but only 1.2 ± 0.07 -fold ($P > 0.05$) in glibenclamide-treated rats. Measuring the areas of hemorrhagic contusion on tissue sections at the epicenter showed that lesions expanded 2.2 ± 0.12 -fold ($P < 0.001$) during the first 24 h in control rats, but only 1.1 ± 0.05 -fold ($P > 0.05$) in glibenclamide-treated rats. Glibenclamide treatment was associated with significantly better neurological function (unilateral BBB scores) at 24 h in both the ipsilateral (median scores, 9 vs 0; $P < 0.001$) and contralateral (median scores, 12 vs 2; $P < 0.001$) hindlimbs.**Conclusion:** MRI is an accurate non-invasive imaging biomarker of lesion expansion and is a sensitive measure of the ability of glibenclamide to reduce lesion expansion.

Spinal Cord advance online publication, 17 September 2013; doi:10.1038/sc.2013.99

Keywords: spinal cord injury; glibenclamide; riluzole; Sur1-Trpm4 channel; MRI; progressive hemorrhagic necrosis

INTRODUCTION

Spinal cord injury (SCI) remains one of the foremost unsolved challenges in medicine. Worldwide, the incidence of SCI ranges from 10 to 83 per million people per year, with half of these patients suffering a complete lesion and one-third becoming tetraplegic.¹ At present, little can be done to undo or repair the initial damage to spinal cord tissues, but great hope lies in reducing secondary injury processes triggered by the primary injury that increase the damage and worsen clinical outcome.

Histological studies on animal models of SCI have shown that early expansion of a hemorrhagic contusion is a common feature following trauma to the spinal cord. During the hours after a blunt impact, a dynamic process ensues wherein a hemorrhagic contusion slowly enlarges, resulting in the progressive autodestruction of spinal cord tissues.^{2–4} Discrete petechial hemorrhages appear, first around the site of injury and then in more distant areas.⁵ As petechial hemorrhages form and coalesce, the lesion gradually expands, with a characteristic region of hemorrhage that ‘caps’ the advancing front of the lesion. A small hemorrhagic lesion that initially involves primarily the capillary-rich gray matter doubles in size during the first 24 h after

injury. The advancing hemorrhage results from delayed progressive catastrophic failure of the structural integrity of capillaries, a phenomenon termed ‘progressive hemorrhagic necrosis’.^{2–4}

Progressive hemorrhagic necrosis has been linked to *de novo* upregulation of sulfonylurea receptor 1 (Sur1)—transient receptor potential melastatin 4 (Trpm4) channels (a.k.a., Sur1-regulated NC_{Ca}-ATP channels)⁶ in microvessels.^{4,7,8} Sur1-Trpm4 channels have been shown to be responsible for the necrotic death of endothelial cells that results in delayed fragmentation of capillaries and formation of petechial hemorrhages. Gene suppression as well as pharmacological blockade of Sur1-Trpm4 channels prevents progressive hemorrhagic necrosis, reduces lesion size and significantly improves neurological function in rodent models of SCI.^{7–10}

To date, the magnitude and time course of lesion expansion due to progressive hemorrhagic necrosis have been characterized in rat models by measuring the amount of extravasated blood in the spinal cords of animals that were killed at different times after trauma.⁴ Although an important measure of injury, quantifying the amount of extravasated blood may not accurately reflect the actual volume of compromised tissue, as this technique cannot distinguish between an

¹Department of Neurosurgery, University of Maryland School of Medicine, Baltimore, MD, USA; ²Department of Pathology, University of Maryland School of Medicine, Baltimore, MD, USA; ³Department of Physiology, University of Maryland School of Medicine, Baltimore MD, USA; ⁴Center for Brain and Spinal Cord Repair and Department of Neuroscience, The Ohio State University College of Medicine, Columbus, OH, USA; ⁵Department of Radiology, University of Maryland School of Medicine, Baltimore MD, USA and ⁶Department of Surgery, Walter Reed Army Medical Center, Washington, DC, USA
Correspondence: Dr JM Simard, Department of Neurosurgery, University of Maryland School of Medicine, 22 South Greene St, Suite 12SD, Baltimore, MD 21201-1595, USA.
E-mail: msimard@smail.umaryland.edu
Received 9 May 2013; revised 1 August 2013; accepted 2 August 2013

increase in the number of erythrocytes within a given volume of tissue versus an actual increase in volume of contused tissue affected by hemorrhage and edema. We hypothesized that magnetic resonance imaging (MRI) could be used to assess early lesion expansion non-invasively and to independently corroborate the existence of early lesion expansion due to progressive hemorrhagic necrosis after spinal cord trauma. Here, we used serial MRI scans obtained at 1 and 24 h after trauma to characterize lesion expansion, and we validated our MRI measurements by comparing them with measurements based on coronal tissue sections in a different group of rats with the same injury. In these experiments, we also examined the effect of glibenclamide on lesion expansion and on neurological function.

MATERIALS AND METHODS

Ethics statement

We certify that all applicable institutional and governmental regulations concerning the ethical use of animals were followed during the course of this research. Animal experiments were performed under a protocol approved by the Institutional Animal Care and Use Committee (IACUC) of the University of Maryland, Baltimore, and in accordance with the relevant guidelines and regulations as stipulated in the United States National Institutes of Health Guide for the Care and Use of Laboratory Animals. All efforts were made to minimize the number of animals used and their suffering. In accordance with 'good laboratory practice', different investigators blinded to injury-group conducted behavioral tests and analyzed the data.

Subjects and experimental series

These experiments were conducted on new series of animals distinct from those previously reported from this laboratory. Thirty-six female Long-Evans rats (250–300 gm; Harlan, Indianapolis, IN, USA) were used in two experimental series (Table 1). In series 1, 12 rats underwent an SCI (see below), six were administered glibenclamide (see below) and six served as untreated controls; these 12 rats were studied using MRI at 1 and 24 h after trauma, after which they were euthanized. In series 2, 24 rats underwent an SCI; eight were euthanized at 15 min; of the remaining 16 rats, eight served as untreated controls and eight were administered glibenclamide; these 16 rats were assessed for locomotor function at 24 h, after which they were euthanized to obtain tissue sections for measurements of the hemorrhagic lesion area at the epicenter.

Sample size calculation

Previous experiments with the model used here suggested that an effect size (Cohen's *d*) of 2.27 (means, 2 vs 1 μ l; pooled s.d., 0.44 μ l) might be expected

for hemorrhage volumes with vehicle vs glibenclamide treatments.⁴ Sample size calculation for a 2-sample comparison ($\alpha = 0.05$; 2-tailed), an effect size of 2.27, and a desired power of 90% indicated a minimum sample size of six per group.

Rat model of SCI

A unilateral impact to the cervical spinal cord at C7 was calibrated to produce ipsilateral but not contralateral primary hemorrhage, resulting in severe SCI, as described in detail previously.^{4,8–10} Female Long-Evans rats (~11 weeks; 250–300 gm; Harlan) were anesthetized (Ketamine, 60 mg kg⁻¹ plus Xylazine, 7.5 mg kg⁻¹, intraperitoneally (IP)). On the left side, the entire lamina of C7 and the dorsal half of the pedicle of C7 were removed. The dura was exposed by removing the interlaminar ligaments rostral and caudal to the lamina of C7 and any remaining ligamentum flavum. The guide tube containing the impactor (1.55-mm tip diameter, 57 mm length, 1.01 gm)¹¹ was angled 5° medially and was positioned using the manipulator arm of the stereotaxic apparatus. The impactor was activated when struck by a 10-gm weight dropped from a height of 25 mm inside the guide tube (velocity, 0.7 m s⁻¹). After injury, rats were nursed on a heating pad to maintain a rectal temperature of ~37 °C and were given 10 ml of glucose-free normal saline subcutaneously. Food and water were placed within easy reach to ensure that the rats were able to eat and drink without assistance. Bladder function was assessed 2–3 times daily by observing for urination, and, if needed, manual emptying of the bladder was carried out using the Credé maneuver.

Treatment

Treatment consisted of the following: (1) administering a single loading dose of glibenclamide (10 μ g kg⁻¹) or an equivalent volume of vehicle IP, at 5 min after trauma; and (2) implanting a mini-osmotic pump (Alzet 2001, 1.0 μ l h⁻¹; Alzet Corp., Cupertino, CA, USA) for continuous subcutaneous infusion of glibenclamide (200 μ g ml⁻¹) beginning at the end of surgery, resulting in delivery of 200 ng h⁻¹ or an equivalent volume of vehicle subcutaneously until euthanasia. This dosing regimen was found previously to significantly ameliorate progressive hemorrhagic necrosis^{8–10} without producing clinically relevant hypoglycemia or any other toxicity.^{4,12,13} Unlike our previous study, in which a 3-h treatment delay was used,⁹ here we used an early treatment time because our principal goal was to validate MRI for measuring early lesion expansion. The formulation of glibenclamide (#G2539; Sigma, St Louis, MO, USA) in dimethyl sulfoxide (DMSO) and the preparation of mini-osmotic pumps have been described in detail.¹⁴ Briefly, a stock solution was prepared by placing 25 mg of glibenclamide into 10 ml of DMSO. The solution used for the loading dose was prepared by adding 4 μ l of stock solution to 1 ml unbuffered normal saline. The solution for infusion was prepared by taking 2.3-ml unbuffered normal saline, adding 4 μ l of 10 N NaOH (undiluted Fixanal; Riedel-deHaën, Seelze, Germany), and then adding 200- μ l stock solution, in that order in order to prevent precipitation of the drug. Control animals received vehicle solution prepared as above but without glibenclamide.

Measurements of primary and secondary hemorrhage

In series 2, at the designated time after injury (15 min for primary hemorrhage; 24 h for primary plus secondary hemorrhage), the rat was anesthetized with sodium pentobarbital (100 mg kg⁻¹), a thoracotomy was performed and the rat was transcardially perfused with normal saline (50 ml) at a pressure of 100 cm H₂O. The spinal cord was collected and sectioned coronally through the epicenter of injury, and the face of the epicenter was imaged at high resolution (1200 dpi) using a flat-bed scanner (Epson Perfection 2450 Photo).

Locomotor function

Basso, Beattie and Bresnahan (BBB) scores were determined as described,¹⁵ except that modifications were introduced to allow more accurate assessment of the functional asymmetry associated with hemicord injury. We refer to this modified functional assessment as modified (unilateral) BBB scores.^{9,10}

Table 1 Experimental series

| Treatment | | Intervention | | |
|-----------|---------------|-------------------|-----|----------------------|
| | | 15 min | 1 h | 24 h |
| Series 1 | | | | |
| Group 1 | Control | | MRI | MRI euthanize |
| (n=6) | | | | |
| Group 2 | Glibenclamide | | MRI | MRI euthanize |
| (n=6) | | | | |
| Series 2 | | | | |
| Group 1 | Control | Euthanize section | | |
| (n=8) | | spinal cord | | |
| Group 2 | Control | | | mBBB score euthanize |
| (n=8) | | | | section spinal cord |
| Group 3 | Glibenclamide | | | mBBB score euthanize |
| (n=8) | | | | section spinal cord |

Abbreviations: mBBB, modified (unilateral) Basso, Beattie and Bresnahan; n, number of rats

Magnetic resonance imaging

In series 1, all rats were imaged 1 and 24 h after trauma; four control rats also were imaged 6 h after trauma. The delay of 1 h in obtaining the 'baseline' MRI was necessitated by logistical considerations, principally the distance between the site where injuries were produced and the site where MRIs were obtained. MRI was performed on a 3.0 Tesla Siemens Trio MR scanner equipped with 18 receiver channels and high performance gradients ($200 \text{ mTm}^{-1} \text{ ms}^{-1}$). An eight-channel wrist coil was used to image the rats. Anesthetized (Ketamine, 60 mg kg^{-1} plus Xylazine, 7.5 mg kg^{-1} , IP) animals were placed in the supine position with the 'sweet spot' of the coil centered on the cervical spine of the rat. The depth of anesthesia was monitored continuously during the imaging session.

The imaging sequences consisted of localizers in the three orthogonal planes. Following localization, T1-weighted magnetization prepared rapid acquisition gradient echo (MP-RAGE) images were acquired in the axial plane with adequate coverage of the injury using 64 slices over a field of view of $53 \text{ mm} \times 62 \text{ mm}$ and an interpolated pixel resolution of 448×512 . The imaging parameters were as follows: inversion time $\text{TI} = 900 \text{ ms}$ and $\text{TE/TR} = 4 \text{ ms}/1900 \text{ ms}$ for an acquisition time of 3 min and 53 s using an acceleration factor of 2. T2-weighted 3D spin-echo images were then acquired in the sagittal and the axial plane. For both planes, the imaging parameters were as follows: $\text{TE/TR} = 93 \text{ ms}/1000 \text{ ms}$, 64 slices, slice thickness 0.3 mm over a field of view of $45 \text{ mm} \times 90 \text{ mm}$ at an interpolated pixel resolution of 312×640 for a total acquisition time of 5 min and 24 s using parallel imaging with an acceleration factor of 2.

All images were reconstructed in three planes to visualize the extent of the lesion. The hemorrhagic portion of the contusion was identified as a hypointense region (due to the presence of hemoglobin) within the cord on T2-weighted images. These regions were demarcated on each slice, and the total volume of the lesion was determined.

Data analysis

T2-hypodensity volumes at 1 versus 24 h were analyzed using Student's paired *t*-test. Areas of hemorrhagic contusion on tissue sections at the epicenter in three groups of rats (15 min untreated, 24-h vehicle, 24-h glibenclamide) were analyzed using AVOVA, with Bonferroni *post hoc* comparisons. Modified (unilateral) BBB scores in two groups of rats (vehicle vs glibenclamide) were analyzed using the Mann-Whitney *U*-test.

RESULTS

In series 1, we evaluated the expansion of the hemorrhagic contusion using serial MRI scans obtained at 1 and 24 h after trauma, with the T2 hypodensity being taken as a measure of extravasated blood.^{16–19} In control rats, a small T2 hypodensity was evident at the first examination, obtained 1 h after trauma (Figure 1a). Subsequent imaging obtained at 6 h ($n = 4$) and 24 h ($n = 6$) confirmed progressive enlargement of the hemorrhagic lesion (Figure 1a). In six control rats, the volume (mean \pm s.e.) of the T2 hypodensity at 1 h after trauma was $1.52 \pm 0.37 \mu\text{l}$, and, after 24 h, the volume increased 2.3-fold to $3.55 \pm 0.87 \mu\text{l}$ ($P < 0.01$) (Figure 1b). By contrast, in six rats treated with glibenclamide 5 min after trauma, the volume of the T2 hypodensity at 1 h was $0.51 \pm 0.21 \mu\text{l}$, and, after 24 h, the volume increased 1.2-fold to $0.59 \pm 0.24 \mu\text{l}$ ($P = 0.43$) (Figure 1b).

In series 2, we evaluated the size of the hemorrhagic contusion using images of tissue sections taken through the epicenter of injury at 15 min and at 24 h. We considered the hemorrhagic area observed at 15 min to represent the primary hemorrhage due to the trauma and the hemorrhagic area observed at 24 h to represent the primary hemorrhage plus the secondary hemorrhage, the latter attributable to progressive hemorrhagic necrosis.

At 15 min, a contusion was apparent that was confined largely to the ipsilateral hemicord, mostly the gray matter (Figure 2a, upper). In control rats, the hemorrhagic contusion at 24 h invariably involved a larger area, typically extending to the contralateral side (Figure 2a,

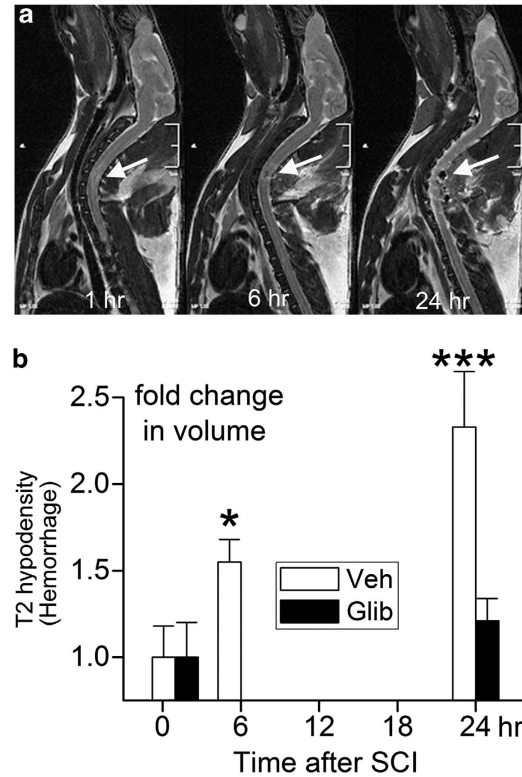


Figure 1 Progressive expansion of hemorrhagic contusion assessed using MRI. (a) Serial MRIs of a control rat obtained at 1, 6 and 24 h after trauma, showing progressive enlargement of the T2 hyperdensity due to the presence of increasing amount of hemoglobin; the data shown are representative of six rats. (b) Fold-change in volumes of T2 hyperdensity measured at the times indicated in control rats (Veh; empty bars) versus glibenclamide-treated rats (Glib; filled bars); mean \pm s.e.; six rats per group; * $P < 0.05$; *** $P < 0.001$.

middle). By contrast, in rats administered glibenclamide 5 min after trauma, the hemorrhagic contusion at 24 h typically occupied an area comparable to that observed at 15 min (Figure 2a, lower). Quantification of the hemorrhagic area showed that, in control rats, lesions were 2.2 ± 0.12 -fold larger at 24 h compared with that at 15 min. By contrast, in glibenclamide-treated rats, lesions were 1.1 ± 0.05 -fold larger at 24 h compared with that at 15 min (Figure 2b).

Commensurate with the favorable effect of glibenclamide on hemorrhagic lesion area, assessment of modified (unilateral) BBB scores at 24 h showed that glibenclamide was associated with significantly better neurological function. Median scores were 0 vs 9 ($P < 0.001$) for the ipsilateral hindlimb and 2 vs 12 ($P < 0.001$) for the contralateral hindlimb, for the control vs glibenclamide groups, respectively (Figure 2c).

DISCUSSION

The principal finding of the present study is that, based on measurements of MRI T2-lesion volume and measurements of hemorrhagic lesion area, there is a 2- to 2.5-fold increase in the hemorrhagic contusion that takes place during the first 24 h after blunt impact trauma to the spinal cord, in good agreement with previous measurements based on tissue hemoglobin.⁴ Previous histological and MRI studies in rats have characterized spinal cord lesions at various times after injury, but relatively few have examined temporal and spatial characteristics of lesion progression during the first hours after injury. To our knowledge, the earliest study

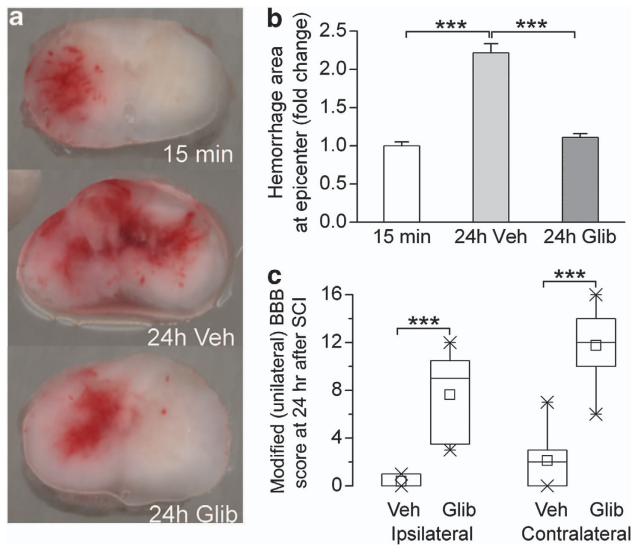


Figure 2 Progressive expansion of hemorrhagic contusion assessed from tissue sections at the epicenter. (a) Representative coronal tissue sections of perfusion-cleared but otherwise unprocessed spinal cords through the epicenter of injury 15 min (top) and 24 h (middle and bottom) after impact, in control rats (top and middle), and in a glibenclamide-treated rat (bottom); the data shown are representative of eight rats per group. (b): Fold-change in areas of hemorrhage at the epicenter in the three groups of rats depicted in (a); mean \pm s.e.; eight rats per group; *** $P < 0.001$. (c) Box plots showing modified (unilateral) BBB scores for the ipsilateral and contralateral hindlimbs at 24 h, for the two groups of rats depicted in (b), 24 h Veh and 24 h Glib; box, 25th and 75th percentiles; \times , 1st and 99th percentiles; line, median; small square, mean.

addressing this question (weight drop; midline, lower thoracic/upper lumbar) reported that, on H&E-stained sections, intramedullary hemorrhages involved an aggregate of 11% of the spinal cord area at the level of maximal bleeding immediately after trauma and that this increased 2.5-fold to 28% after 8 h.²⁰ In our previous study (weight drop; lateral C7), we reported a twofold increase in the amount of extravasated blood in tissues from the epicenter during the first 12 h after trauma.⁴ In an MRI study (0.5 mm compression for 30 msec; T7), the T2-lesion volume was found to expand ~ 1.5 -fold over 5.5 h.¹⁶ Together with the present study, these various animal studies using different methods establish conclusively the existence of significant lesion expansion during the early hours after blunt impact to the spinal cord. Recently, lesion expansion also was demonstrated using serial MRI scans in humans with cervical SCI.²¹ The importance of these observations lies in the hope that, if early lesion expansion can be halted, patients with acute SCI may suffer the least possible secondary injury.

The model of cervical hemicord impact that we used here is particularly well suited to examining the expansion of the primary injury to the contralateral side. In this model, care is taken to obtain a primary hemorrhage exclusively ipsilateral to the site of impact. This model emphasizes the distinction between primary and secondary hemorrhage, and it shows the influence of secondary hemorrhage on outcome.⁸ When primary hemorrhage is located exclusively unilaterally, subsequent spread of the hemorrhagic lesion to the contralateral side during the ensuing hours—by definition, secondary hemorrhage—is readily discerned both histologically and functionally. Moreover, if the primary hemorrhage is confined to one side and if secondary expansion of the hemorrhagic lesion to the contralateral side is prevented, the magnitude and importance of secondary

hemorrhage is readily appreciated. By contrast, with bilateral primary hemorrhage, neurological dysfunction due to secondary hemorrhage is more difficult to detect. When the primary hemorrhage already occupies most of a spinal segment, expansion laterally of secondary hemorrhage may be limited or functionally mute. Rostro-caudal expansion would still occur but, depending on the spinal cord level involved, for example, cervical vs thoracic, this may be difficult to detect neurologically.

An important aspect of the present study is that it confirmed previous observations that early lesion expansion can be prevented by blocking either of the two subunits of the Sur1-Trpm4 channel.⁶ Lesion expansion is prevented by blocking Sur1, either pharmacologically with glibenclamide or repaglinide,⁴ or by gene suppression with antisense oligodeoxynucleotide or gene deletion of *Abcc8*,⁸ or by blocking Trpm4, either pharmacologically with flufenamic acid⁷ or riluzole,⁹ or by gene suppression with antisense oligodeoxynucleotide or gene deletion of *Trpm4*.⁷

In the present study examining acute outcomes at 24 h, in three other series from our laboratory examining outcomes at 1 or 6 weeks,^{4,8,10} and in one series from an independent laboratory,²² glibenclamide treatment beginning shortly after trauma was found to be highly effective in reducing lesion size and improving neurological function. In a 6th series of rats with outcomes evaluated at 6 weeks, treatment at the clinically more relevant time of 3 h after trauma also was found to be highly beneficial.⁹ As might be expected, the magnitude of the benefit observed with glibenclamide depends on the magnitude of the primary injury,¹⁰ but all studies to date examining functional outcome and lesion size at 6 weeks have demonstrated a significant treatment effect, regardless of the initial severity.^{8–10}

In the 6 series to date with glibenclamide, drug was delivered by constant subcutaneous infusion. From a pharmacokinetic perspective, cutaneous delivery of glibenclamide is highly effective for maintaining steady plasma levels, is superior to enteral administration and appears to be equivalent to intravenous (IV) administration.²³ Constant subcutaneous infusion of glibenclamide was used in the preclinical studies as a convenient alternative to constant IV infusion, as is used with injectable glibenclamide (RP-1127) in clinical trials for other CNS indications (ClinicalTrials.gov identifiers: NCT01454154; NCT01268683; NCT01794182). In the animal studies, no clinically relevant hypoglycemia or other toxicity has been detected with infusions of 200 ng h^{-1} ,^{4,12,13} or 400 ng h^{-1} .²⁴ In a Phase I trial of RP-1127 in 16 healthy volunteers (ClinicalTrials.gov identifier: NCT01132703), a 3-day IV infusion ($125 \mu\text{g/h}$) produced no clinically significant hypoglycemia or other serious adverse event (S. Jacobson, personal communication).

A recent comprehensive review²⁵ shows how difficult it can be to translate preclinical trials on acute pharmacotherapeutic neuroprotection to clinical trials in SCI. Among numerous challenges, consideration must be given to the accumulated preclinical data on any proposed therapeutic agent as well as the effect of that agent on surrogate end points and functional outcome. The work reported here shows that early MRI may be a useful imaging biomarker of lesion expansion, a phenomenon that is prominent in human SCI,²¹ and that may serve as a useful proxy for treatment efficacy.

Riluzole has been found to be efficacious in preclinical models of SCI,^{9,26,27} may have a beneficial effect on motor outcome in cervical SCI, as recently reported in a small open-label Phase I clinical trial,²⁸ and is planned for study in a Phase II clinical trial of acute SCI (ClinicalTrials.gov identifier, NCT01597518). A recent preclinical study using a rat model of SCI, which was so severe as to have

attendant mortality, compared treatment with riluzole (2.5 mg kg⁻¹ IP every 12 h × 1 week) vs glibenclamide (200 ng h⁻¹ continuous subcutaneous infusion – 1 week), starting 3 h after trauma.⁹ This study found that glibenclamide is superior to riluzole in terms of both toxicity and efficacy. Riluzole exhibits a peculiar, dose-limiting CNS toxicity in the context of CNS trauma that is absent in non-injured controls: in SCI, mortality rates of 0, 8 and 70% were observed with 4, 6 and 8 mg kg⁻¹ IP every 12 h, respectively.²⁷ Riluzole is a pleiotropic drug with inhibitory effects on sodium channels, glutamatergic pathways and Trpm4.⁹ However, the near-identity of the phenotypes observed with riluzole⁹ compared with gene suppression of Sur1⁸ as well as gene suppression of Trpm4⁷ suggests that a major effect of riluzole in SCI is via inhibition of the Sur1-Trpm4 channel. Glibenclamide appears to be a safer choice than riluzole for targeting the Sur1-Trpm4 channel in acute CNS injury.

The present study has important shortcomings. First, it was not designed as an efficacy study, but rather to demonstrate the concept that MRI could be used to measure progressive lesion expansion in a rat model of SCI. Thus, the number of subjects studied was small, although the specific number was determined by a power analysis. The most important shortcoming was that the first MRI was obtained 1 h after trauma, whereas treatment with glibenclamide was administered 5 min after trauma. The long delay in obtaining the MRI was necessitated by logistical considerations, principally the distance between the site where injuries were produced and the site where MRIs were obtained. We believe that this problem with study design is the reason for the apparently smaller ‘baseline’ lesions in glibenclamide versus control groups, even though both groups were injured in the same way. Further experiments will be needed to examine MRIs at earlier times. However, if our interpretation is correct, it suggests that ‘hyper-early’ treatment with glibenclamide may be highly desirable for maximally improving outcome.

In conclusion, the present study reaffirms that early enlargement of the hemorrhagic contusion is an important factor determining outcome in SCI, and that reducing early enlargement of the hemorrhagic contusion with glibenclamide can contribute significantly to improved functional outcome.

DATA ARCHIVING

There were no data to deposit.

CONFLICT OF INTEREST

JMS holds a US patent (7,872,048), ‘Methods for treating spinal cord injury with a compound that inhibits a NC(Ca-ATP) channel’. JMS is a member of the scientific advisory board and holds shares in Remedy Pharmaceuticals. No support, direct or indirect, was provided to JMS, or for this project, by Remedy Pharmaceuticals. All other authors declare no conflict of interest.

ACKNOWLEDGEMENTS

This work was supported by grants to JMS from the Department of Veterans Affairs (Baltimore) and from the National Institute of Neurological Disorders and Stroke (NINDS) (NS060801); to VG from NINDS (NS061934); to PGP from NINDS (HHSN271200800040C) and from the Ray W. Poppleton endowment (OSU); and to PGP and JMS from the Department of the Army (W81XWH 1010898).

- Steward O, Schauwecker PE, Guth L, Zhang Z, Fujiki M, Inman D *et al*. Genetic approaches to neurotrauma research: opportunities and potential pitfalls of murine models. *Exp Neurol* 1999; **157**: 19–42.
- Guth L, Zhang Z, Steward O. The unique histopathological responses of the injured spinal cord. Implications for neuroprotective therapy. *Ann N Y Acad Sci* 1999; **890**: 366–384.
- Simard JM, Tsybalyuk O, Ivanov A, Ivanova S, Bhatta S, Geng Z *et al*. Endothelial sulfonyleurea receptor 1-regulated NC(Ca-ATP) channels mediate progressive hemorrhagic necrosis following spinal cord injury. *J Clin Invest* 2007; **117**: 2105–2113.
- Kawata K, Morimoto T, Ohashi T, Tsujimoto S, Hoshida T, Tsunoda S *et al*. Experimental study of acute spinal cord injury: a histopathological study. *No Shinkei Geka* 1993; **21**: 45–51.
- Woo SK, Kwon MS, Ivanov A, Gerzanich V, Simard JM. The sulfonyleurea receptor 1 (Sur1)-transient receptor potential melastatin 4 (Trpm4) channel. *J Biol Chem* 2013; **288**: 3655–3667.
- Gerzanich V, Woo SK, Vennekens R, Tsybalyuk O, Ivanova S, Ivanov A *et al*. De novo expression of Trpm4 initiates secondary hemorrhage in spinal cord injury. *Nat Med* 2009; **15**: 185–191.
- Simard JM, Woo SK, Norenberg MD, Tosun C, Chen Z, Ivanova S *et al*. Brief suppression of Abcc8 prevents autodestruction of spinal cord after trauma. *Sci Transl Med* 2010; **2**: 28a29.
- Simard JM, Tsybalyuk O, Keledjian K, Ivanov A, Ivanova S, Gerzanich V. Comparative effects of glibenclamide and riluzole in a rat model of severe cervical spinal cord injury. *Exp Neurol* 2012; **233**: 566–574.
- Simard JM, Popovich PG, Tsybalyuk O, Gerzanich V. Spinal cord injury with unilateral versus bilateral primary hemorrhage—effects of glibenclamide. *Exp Neurol* 2012; **233**: 829–835.
- Soblosky JS, Song JH, Dinh DH. Graded unilateral cervical spinal cord injury in the rat: evaluation of forelimb recovery and histological effects. *Behav Brain Res* 2001; **119**: 1–13.
- Simard JM, Chen M, Tarasov KV, Bhatta S, Ivanova S, Melnitchenko L *et al*. Newly expressed SUR1-regulated NC(Ca-ATP) channel mediates cerebral edema after ischemic stroke. *Nat Med* 2006; **12**: 433–440.
- Simard JM, Yurovsky V, Tsybalyuk N, Melnichenko L, Ivanova S, Gerzanich V. Protective effect of delayed treatment with low-dose glibenclamide in three models of ischemic stroke. *Stroke* 2009; **40**: 604–609.
- Simard JM, Woo SK, Tsybalyuk N, Voloshyn O, Yurovsky V, Ivanova S *et al*. Glibenclamide-10-h treatment window in a clinically relevant model of stroke. *Transl Stroke Res* 2012; **3**: 286–295.
- Basso DM, Beattie MS, Bresnahan JC. A sensitive and reliable locomotor rating scale for open field testing in rats. *J Neurotrauma* 1995; **12**: 1–21.
- Bilgen M, Abbe R, Liu SJ, Narayana PA. Spatial and temporal evolution of hemorrhage in the hyperacute phase of experimental spinal cord injury: in vivo magnetic resonance imaging. *Magn Reson Med* 2000; **43**: 594–600.
- Hackney DB, Ford JC, Markowitz RS, Hand CM, Joseph PM, Black P. Experimental spinal cord injury: MR correlation to intensity of injury. *J Comput Assist Tomogr* 1994; **18**: 357–362.
- Ohta K, Fujimura Y, Nakamura M, Watanabe M, Yato Y. Experimental study on MRI evaluation of the course of cervical spinal cord injury. *Spinal Cord* 1999; **37**: 580–584.
- Weirich SD, Cotler HB, Narayana PA, Hazle JD, Jackson EF, Coupe KJ *et al*. Histopathologic correlation of magnetic resonance imaging signal patterns in a spinal cord injury model. *Spine* 1990; **15**: 630–638.
- Balentine JD. Pathology of experimental spinal cord trauma. I. The necrotic lesion as a function of vascular injury. *Lab Invest* 1978; **39**: 236–253.
- Aarabi B, Simard JM, Kufera JA, Alexander M, Zacherl KM, Mirvis SE *et al*. Intramedullary lesion expansion on magnetic resonance imaging in patients with motor complete cervical spinal cord injury. *J Neurosurg Spine* 2012; **17**: 243–250.
- Popovich PG, Lemeshow S, Gensel JC, Tovar CA. Independent evaluation of the effects of glibenclamide on reducing progressive hemorrhagic necrosis after cervical spinal cord injury. *Exp Neurol* 2012; **233**: 615–622.
- Mishra MK, Ray D, Barik BB. Microcapsules and transdermal patch: a comparative approach for improved delivery of antidiabetic drug. *AAPS Pharm Sci Tech* 2009; **10**: 928–934.
- Tosun C, Koltz MT, Kurland DB, Ijaz H, Gurakar M, Schwartzbauer G *et al*. The Protective Effect of Glibenclamide in a Model of Hemorrhagic Encephalopathy of Prematurity. *Brain Sci* 2013; **3**: 215–238.
- Tator CH, Hashimoto R, Raich A, Norvell D, Fehlings MG, Harrop JS *et al*. Translational potential of preclinical trials of neuroprotection through pharmacotherapy for spinal cord injury. *J Neurosurg Spine* 2012; **17** (Suppl I), 157–229.
- Wahl F, Stutzmann JM. Neuroprotective effects of riluzole in neurotrauma models: a review. *Acta Neurochir Suppl* 1999; **73**: 103–110.
- Wu Y, Satkunendrarajah K, Teng Y, Chow DS, Buttigieg J, Fehlings MG. Delayed post-injury administration of riluzole is neuroprotective in a preclinical rodent model of cervical spinal cord injury. *J Neurotrauma* 2013; **30**: 441–452.
- Grossman RG, Fehlings M, Frankowski R, Burau KD, Chow D, Tator C *et al*. A prospective multicenter phase 1 matched comparison group trial of safety, pharmacokinetics, and preliminary efficacy of riluzole in patients with traumatic spinal cord injury. *J Neurotrauma* (e-pub ahead of print 16 July 2013).



This work is licensed under a Creative Commons Attribution 3.0 Unported License. To view a copy of this license, visit <http://creativecommons.org/licenses/by/3.0/>

1 Wyndaele M, Wyndaele JJ. Incidence, prevalence and epidemiology of spinal cord injury: what learns a worldwide literature survey? *Spinal Cord* 2006; **44**: 523–529.